

**DECONTAMINATION EFFICACY
OF GRAPHENE OXIDE AND
SILANIZED GRAPHENE OXIDE BASED
TOPICAL PICKERING EMULGELS FOR THE
REMOVAL OF HEAVY METAL IONS**

**A Thesis Submitted
in Partial Fulfilment of the Requirements
for the Degree of
MASTER OF PHARMACY**

**in
Pharmaceutics
by
SAUMYA TOMER
(Enrollment no. 2202270566005)**

Under the Supervision of

**Supervisor:
Mrs. Roshan Zehra
Associate Professor**

**Co- Supervisor:
Mrs. Sandhya Sharma
Assistant Professor**

Innovative College of Pharmacy



to the

Faculty of Pharmacy

**DR. A.P.J. ABDUL KALAM TECHNICAL UNIVERSITY
(Formerly Uttar Pradesh Technical University) LUCKNOW**

(July, 2024)

DECLARATION

I hereby declare that the research work entitled "**Decontamination efficacy of grapheneoxide and silanized graphene oxide based topical Pickering emulgels for removal of heavy metal ions.**" embodied in this thesis for the award of Degree of **Masters in Pharmacy in Pharmaceutics** is original work and was carried out in INMAS, DRDO, New Delhi under the supervision and guidance of **Dr. Himanshu Ojha (Sci. "F")**. I also declare that the matter embodied in it is original and the same has not previously formed the basis for the award of any degree of any other university or institution.

Saumya Tomer

Enrollment No. - 2202270566005

Innovative College of Pharmacy
Greater Noida, Uttar Pradesh-201308

DECONTAMINATION EFFICACY OF GRAPHENE OXIDE AND SILANIZED GRAPHENE OXIDE BASED TOPICAL PICKERING EMULGELS FOR REMOVAL OF HEAVY METAL IONS

Saumya Tomer

ABSTRACT

This research work aimed to assess the decontamination efficacy of graphene oxide (GO) and silanized graphene oxide (sGO) based topical Pickering emulgels for removal of heavy metal ions. Emulgel as a topical dosage form used for the controlled release of emulsion and gel in combined form. Pickering emulgels use solid particles as stabilizers, which accumulate at the interface between two immiscible liquids and stabilize droplets against coalescence. GO is a layered carbon structure with oxygen-containing functional groups that acts as a nanocarrier in various applications such as drug delivery systems, gene delivery, biological sensing etc. sGO was synthesized from GO using APTES as the silane precursor. GO and sGO were characterized by FT-IR, TGA, FE-SEM and Raman spectroscopy. Further, adsorptive removal of heavy metal ions by GO and sGO was investigated using AAS and complexation analysis was done by fluorescence spectroscopy which indicated that GO and sGO have good adsorption efficacy. The PE was synthesized using GO and sGO as a decontaminating agent in the formulation. The formulated PE was characterized based on its physical appearance, pH, viscosity and rheological properties, DSC, contact angle, FT-IR, zeta potential, FE-SEM, and stability studies. The contact angle determination showed that PE prepared is of oil in water type. Rheological studies indicated that the formulated emulgel has non-newtonian and shear-thinning flow behavior. Furthermore, the skin decontamination efficacy of PE will be evaluated in future using SD rats.

Keywords: Graphene oxide, Pickering emulgel, Adsorption, Decontamination

ACKNOWLEDGEMENT

I am very thankful to **Institute of Nuclear Medicine and Allied Sciences (INMAS), DRDO, Delhi** for providing me an opportunity for doing my dissertation work.

I would also like to thank **Dr. Sudhir Chandana Sci. "G", Director, INMAS, DRDO** for giving me this opportunity to work at this prestigious institution. I wish to express my heartiest thanks to **Mr. Vinod Kaushik Sci. "F", Head of the Department, CBRN, INMAS, DRDO**. I would like to sincerely thanks to my collaborating supervisor **Dr. Himanshu Ojha Sci. "F", Division of CBRN, INMAS, DRDO** for their continuous support and fulfilment of my dissertation work. The faith that my internal supervisor and external supervisor have shown on me was a major inspiration in what I have achieved during my dissertation work. The art of converting the failure to success through hard work and dedication.

I am sincerely grateful for the help I received in this dissertation work. I would like to acknowledge with extreme gratitude to **Dr. Amarjeet Singh, Principal of Innovative College of Pharmacy**, and my supervisor **Mrs. Roshan Zehra, Associate Professor** and **Mrs. Sandhya Sharma, Assistant Professor**, Faculty of Innovative College of Pharmacy, AKTU, Greater Noida, Uttar Pradesh for their guidance and support at each step.

I wish to express my sincere thanks to my seniors **Ms. Lajpreet Kaur, Ms. Ayushi Mishra** and **Mr. Piyush Verma** for their genuine help and kind support during my dissertation work. I'm especially grateful to Ms. Lajpreet Kaur for her guidance, valuable suggestions, and encouragement that were crucial in helping me in completing my research work. I am very grateful for their willingness to share their knowledge and experience, which greatly improved my understanding and skills. Their constructive feedback and continuous motivation have been a great source of inspiration for me. I truly appreciate their patience, cooperation, and unwavering support throughout the journey making it enriching and fulfilling.

I would also like to extend huge, warm thanks to my friends **Manish Saini, Koushika Parida, Sanket Mathwale, Sheetal Gulia** and **Anjali Sharma** for their support and ever needed cooperation. The time spent with them was mesmerizing and memorable and will remain in my heart throughout my life.

I would like to pay my deep regards to my parents and my younger sister for their unconditional love, support and blessings due to which this work reached to the completion. Once again, I would like to thank all those who were directly and indirectly involved in the completion of the project.

SAUMYA TOMER

TABLE OF CONTENTS

	Page No.
Certificate-I	ii
Declaration	iii
Abstract	iv
Acknowledgement	v-vi
List of Tables	x
List of Figures	xi-xii
List of Abbreviations	xiii
CHAPTER 1: INTRODUCTION	1-12
1.1 Nuclear weapons1-2	
1.1.1 General introduction	1
1.1.2 Mortalities due to nuclear weapons1	
1.1.3 Hazards relating to nuclear waste or weapons1-2	
1.2 Heavy metal ion toxicity2-7	
1.2.1 General	2
1.2.2 Toxicity and risks due to heavy metals2-3	
1.2.2.1 Diseases due to toxicity	
1.2.2.2 Hazards due to army or military operations	
1.2.3 Cobalt	3-4
1.2.3.1 General	
1.2.3.2 Health Hazards	
1.2.4 Strontium	4-5
1.2.4.1 General	
1.2.4.2 Health Hazards	
1.2.5 Removal of heavy metal ions	5-7
1.3 Pickering emulgel 7-9	
1.3.1 General	7
1.3.2 Emulgel	7-8
1.3.2.1 Types of emulgels	9
1.3.3 Pickering emulgel	8-9
1.4 Decontamination of skin 9-12	
1.4.1 Skin	9
1.4.1.1 Structure of skin	
1.4.2 Decontamination	10-12
1.4.2.1 Types of decontamination	
1.4.2.2 Methods of decontamination	
1.4.2.3 Selection of suitable decontaminants	

1.4.2.4 Commercially available formulations

CHAPTER 2: REVIEW OF LITERATURE13-22

CHAPTER 3: AIM AND OBJECTIVES23-24

3.1 Aim	23
3.2 Objectives	23
3.3 Plan of Work	23-24
3.4 Rationale	24

CHAPTER 4: DRUG PROFILE 25-29

4.1 Drug's Profile	25-26
4.2 Excipients Profile	26-29

CHAPTER 5: INSTRUMENTATION, MATERIALS AND METHODOLOGY

5.1 Instrumentation 29-36

5.1.1 Fluorescence spectroscopy	29-30
5.1.2 Fourier Transform Infrared Spectroscopy	31-33
5.1.3 Atomic absorption spectroscopy	33-35
5.1.4 UV-Vis Spectroscopy	35-36

5.2 Materials 37-38

5.2.1 List of chemicals/reagents	
5.2.2 List of glasswares and plasticware	

5.3 Methodology 38-46

5.3.1 Synthesis of sGO from GO39	
5.3.2 Pre-formulation study of GO and sGO	
5.3.2.1 FT-IR	
5.3.2.2 Thermogravimetric analysis	
5.3.2.3 Field emission scanning electron microscopy	
5.3.2.4 Raman spectroscopy	
5.3.3 Adsorptive removal of heavy metal ions	40-41
5.3.3.1 By AAS	
5.3.3.2 By Fluorescence spectroscopy	
5.3.4 Synthesis of GO and sGO based pickering emulgels	41-42
5.3.5 Characterization of GOPE and sGOPE	42-45
5.3.5.1 Physical Appearance	
5.3.5.2 pH Determination	
5.3.5.3 Particle Size Analysis	
5.3.5.4 Zeta Potential	
5.3.5.5 Optical Microscopy	
5.3.5.6 Rheological Studies	
5.3.5.7 Differential Scanning Calorimetry (DSC)	
5.3.5.8 FT-IR	

5.3.5.9 Contact Angle Measurement	
5.3.5.10 FE-SEM	
5.3.5.11 Stability Studies	
5.3.6 Decontamination studies	46
5.3.6.1 Preparation of animals	
5.3.6.2 Decontamination procedure	
CHAPTER 6: RESULTS AND DISCUSSION	48-65
CHAPTER 7: CONCLUSION	66-68
CHAPTER 8: FUTURE PROSPECTS	69-70
CHAPTER 9: REFERENCES	

LIST OF TABLES

Table No.	Title	Page No.
5.1	List of chemicals/reagents	37
5.2	List of instruments	37
5.3	List of glasswares and plasticwares	38
6.1	FTIR peaks of GO	48
6.2	FTIR peaks of sGO	49
6.3	Physical and chemical properties of emulgel	56
6.4	FT-IR peaks corresponding to different functional groups of various components of PE	61
6.5	Stability study analysis of GOPE and sGOPE	64-65

LIST OF FIGURES

Figure No.	Title	Page No.
4.1	Structure of Graphene oxide	25
4.2	Structure of silanized graphene oxide	26
4.3	Structure of diethyl adipate	26
4.4	Structure of kolliphorel	27
4.5	Structure of xanthum gum	28
4.6	Structure of glycerol	
5.1	Fluorescence Spectrometer	29
5.2	Fourier Transform Infrared Spectrometer	31
5.3	Atomic Absorption Spectrophotometer	33
5.4	UV-Vis Spectrophotometer	35
5.6	Synthesis of sGO	38-39
5.7	Steps for synthesis of GOPE/sGOPE	42
6.1	FTIR spectra of GO	48
6.2	FTIR spectra of sGO	49
6.3	TGA of GO and sGO	50
6.4	FE-SEM images of (a) GO and (b) sGO	51
6.5	Raman spectra of (a) GO and (b) sGO	51
6.6	Effect of dose on adsorptive efficacy of sGO for $\text{Co}^{+2}/\text{Sr}^{+2}$	52
6.7	Effect of contact time on adsorption efficacy of sGO for $\text{Co}^{+2}/\text{Sr}^{+2}$	53

6.8	Fluorescence spectra of sGO with cobalt ions	54
6.9	Fluorescence spectra of sGO with strontium ions	54
6.10	Appearance of GOPE and sGOPE	55
6.11	Size analysis of (a) GOPE and (b) sGOPE	56
6.12	Zeta Potential of (a) GOPE and (b) sGOPE	57
6.13	Optical microscopic images of (a) GOPE and (b) sGOPE	57
6.14	Flow curves of GOPE	58
6.15	Flow curves of sGOPE	58
6.16	Frequency sweep plots of GOPE and sGOPE	59
6.17	Amplitude sweep plots of GOPE and sGOPE	59
6.18	DSC curves of (a) GOPE and (b) sGOPE	60
6.19	FTIR spectra of GOPE, sGOPE and all the components of emulgel	62
6.20	Contact angles of (a) GOPE and (b) sGOPE	62
6.21	FE-SEM images of (a) GOPE and (b) sGOPE at 5X magnification and 50X magnification	63

LIST OF ABBREVIATIONS

GO	Graphene Oxide
sGO	Silanized graphene oxide
PE	Pickering emulgel
GOPE	Graphene oxide pickering emulgel
sGOPE	Silanized graphene oxide pickering emulgel
Co	Cobalt
Sr	Strontium
Cs	Cesium
APTES	(3-Aminopropyl) triethoxysilane
FTIR	Fourier Transform Infrared Spectroscopy
XRD	X-ray diffraction
SEM	Scanning electron microscopy
DLS	Dynamic Light Scattering
AAS	Atomic absorption spectroscopy

CHAPTER-1

INTRODUCTION

CHAPTER-1

INTRODUCTION

1.1 NUCLEAR WEAPONS

1.1.1 General

The finish of The Second Great War marked the beginning of the atomic age, prompting many nations to engage in an atomic weapons contest. Between 1945 & 1964, the US, USSR, United Kingdom, France, and China each created atomic weapons. By early 2022, there were approximately 13,000 nuclear warheads distributed among nine countries. The threat posed by nuclear weapons has escalated due to increased proliferation, the risk of terrorism, and ongoing political instability (Xu & Dodt, 2023)[78].

1.1.2 Mortalities due to nuclear weapons

Atomic Bombings of Hiroshima and Nagasaki: Roughly 140,000 people in Hiroshima (1945) & 73,000 in Nagasaki (1945) passed on either instantly or in no less than five months because of the consolidated impacts of blast pressure, radiant heat, and ionizing radiation produced by nuclear fissions. (Tomonaga, 2019)[68]. The thermal energy station mishaps at Three Mile Island (1979), Chernobyl (1986), & Fukushima (2011) saw 134 individuals develop acute radiation syndrome (ARS) from direct radiation exposure. There were 28 immediate fatalities, with 95% occurring at whole body. By the end of the year 2001, an additional 14 ARS survivors had died from various causes (De Cauwer et al., 2023)[20]. **A dirty bomb**, also known as a radiological weapon, represents the simplest and least sophisticated form of nuclear terrorism. Various radioisotopes can be used in a dirty bomb, with those that are relatively accessible, have long half-lives, and emit strong radiation being the most likely candidates. Examples include iridium-192, cobalt-60, and caesium-137. Strontium-90, which accumulates in bone (Barnaby Research et al., 2005)[60].

1.1.3 Hazards relating to nuclear waste or weapons

When radioactive material is uniformly spread as an aerosol (tiny particles) in an area it

can lead to skin contamination from the airborne particles. The primary concern is the immediate health effects from skin contact with the radiation, with a high dose rate (> 1.25 Sv/hr) causing acute health issues. Strontium-90 and Cesium-137 are the two isotopes most likely to be used in this type of attack due to their significant radiation effects on the skin (Curling, 2016)[16]. The extensive use of nuclear technology, the nuclear industry, mining, and petroleum exploration have all contributed to the creation of radioactive waste containing isotopes like ^{60}Co , ^{137}Cs , and ^{90}Sr , among others (Zhuang & Wang, 2023)[80]. Furthermore, the chances of Sr and Co emissions into the environment has grown due to advancements in modern technologies.

1.2 HEAVY METAL IONS

1.2.1 General

Weighty metals are for the most part characterized as metals with a thickness more noteworthy than 5 g/cm^3 , and they are known to have detrimental effects on the climate and living organic entities. Included metals are crucial for sustaining different biochemical and physiological functions in living organic entities at trace concentrations, but they become dangerously toxic when they exceed certain thresholds (Jaishankar et al., 2014)[38]. They tend to bind to protein sites not designated for them, displacing native metals from their natural binding sites, which disrupts cell function and leads to toxicity (Jaishankar et al., 2014)(Skalny et al., 2021)[38][62].

1.2.2 Toxicity and risks due to heavy metals

1.2.2.1 Diseases due to toxicity

Heavy metals toxicity can decrease energy levels and pose harmful effects on mind, lungs, kidneys, liver, blood creation, and other crucial organs. Long haul openness can cause slowly progressing physical, solid, and neurological degeneration, same to diseases like various sclerosis, Parkinson's sickness, Alzheimer's illness, and strong dystrophy. Repeated prolonged openness to certain metals & their mixtures can also cause cancer (Järup, 2003)[39].

1.2.2.2 Hazards due to army or military operations

Outfitted clashes and military exercises add to ecological contamination from metals. The results in contamination of the environment, various exposure routes, and associated health risks. Military activities have led to human exposure to heavy metals

through inward breath or ingestion of metal particles and wounds from inserted metal parts leading to adverse neurological, cardiovascular, reproductive effects, respiratory, ocular and neurodevelopmental disorders (*Shukla 2023.Pdf*, n.d.)[61]. Military operations, such as live terminating exercises, training activities, garbage removal, and foundation support, have hurt soil, water, and air (Edwards, 2002) #Trovo et al., .2017 [27][70]. During military operations, gunshot residue (GSR) released after firing contains numerous metal particles that in the long run arrive at the climate Charles et al., 2020[13]. Various weapons residues, including those from artillery, grenades, pistols, revolvers, rifles, and rockets, contribute to environmental pollution (Gruss et al., 2019)[35].

Inward breath of harmful vapor produced during terminating is the essential course of openness, causing several adverse health hazards. A study on 236 Iran-Bay Conflict warriors indicated that about seventy eight% of veterans experienced respiratory difficulties within 2 to 28 months of their service in the affected area (*Shukla 2023.Pdf*, n.d.)[61]. Additionally, military personnel were presented to sarin and cyclosarin during the disposal of an ammo stockroom in Iraq which brought about inward breath and contact with the skin and eyes causing toxicities (Darchini-Maragheh et al., 2018)(Etemad et al., 2018)[19][30].

Military personnel face high risks from weapons due to occupational exposure. Major risks involve handling of bombs and various weapons such as grenades, missiles, rockets, rifles, pistols, and revolvers. Painful wounds induced during war can become contaminated with toxic metals and other substances, leading to wellbeing gambles from both intense and constant openness because of installed sections (*Shukla 2023.Pdf*, n.d.)[61].

1.2.3 Cobalt

1.2.3.1 General

Cobalt is ubiquitous in natural environment and can be originated as an effect of anthropogenic activity. This element is used in several nuclear power plants and industrial applications. It is one of the fundamental minor components for the human body and can exist in both organic and inorganic forms (Donald Barceloux & Barceloux, 1999)[23]. It is a crucial cofactor in cell division and a key component of

vitamin B12 (hydroxocobalamin). It assumes a significant part in the formation of proteins and amino acids that create the myelin sheath around nerve cells. A lack of cobalt can disrupt the production of vitamin B12, potentially leading to anaemia, hypothyroidism, and increasing the risk of developmental issues in infants. Conversely, an excess of cobalt can overstimulate the thyroid and bone marrow, potentially causing conditions like excessive red blood cell production, pulmonary fibrosis, and asthma (Czarnek et al., 2015)(Abdel-Raouf et al., 2022)[1][17].

1.2.3.2 Health Hazards

In nuclear power plants, cobalt can exist in two radioactive forms i.e. ^{58}Co and ^{60}Co . It is a metal pollutant that enters the environment mostly through human actions. Cobalt is typically released into water by mining, pigment production, nuclear reactors, plastic and catalytic processes, alloys, and numerous other industries. Excess of it in the body can have negative effects include allergies resembling asthma, irregular heartbeats that result in heart failure, and damage to the thyroid and liver (Yusof et al., 2019)[79]. However, an excessive release of ^{60}Co into the environment would result in paralysis and diarrhoea due to the high intensity gamma rays emitted by it and its comparatively long half-life (Ouyang et al., 2020)[52]. Human memory loss may be brought on by cobalt, which is also known to produce neurotoxicity in animal studies (Tayyebi et al., 2015)[67]. Exposure to cobalt can cause an allergic dermatitis similar to nickel dermatitis, characterized by erythematous papules and the typical symptoms of urticaria, even with minimal exposure (Benson et al., 1975)(Payne, 1977)[9][53].

1.2.4 Strontium

1.2.4.1 General

Strontium, an alkaline earth metal having chemical similarities with barium and calcium, is not considered essential for human or animal life (Ali et al., 2020)[5]. However, its presence in the environment poses significant hazards due to the radioactive nature of its isotopes (Chowdhury & Blust, 2011)[15]. The primary sources of these isotopes are from military and civilian nuclear programs, which includes activities such as nuclear weapon testing, power generation, and medical and industrial applications utilizing radioactive nuclides (Amer et al., 2017)[7].

1.2.4.2 Health hazards

Accumulation of radioactive strontium isotopes, particularly ^{89}Sr and ^{90}Sr , in bone tissue poses health risks to both humans and animals. These isotopes, with half-lives of 51 days and 29 years respectively, are generated during the reprocessing of nuclear fuel rods and as byproducts of nuclear fission in power plants (Ali et al., 2020)(Koilaraj et al., 2018)[5][44]. Due to its long lifespan, high solubility, and bio-toxicity, the separation and recovery of strontium from waste solutions require special attention (Ahmadpour et al., 2010)[2]. One of the major challenges we face today is managing, treating, and disposing of radioactive waste. Due to their similar biological properties to calcium, strontium can infiltrate the body, leading to serious health issues such as leukaemia and bone tumours. It can harm the skeleton and influence the hematopoietic tissue in the bone marrow, underscoring the urgent need for effective strategies to handle radioactive waste (Xing et al., 2019)[77].

Significant quantities of ^{90}Sr were discharged into aquatic environments due to the nuclear incidents at Chernobyl (Sr., deliver into the air) and Fukushima (Sr., deliver into sea)Daiichi (Vipin et al., 2016)(Amer et al., 2017)[7][73]. A critical challenge in nuclear waste management is the remediation of radioactive wastewater generated by commercial nuclear power reactors. Effective removal of strontium radionuclides from wastewater prior to its release into natural water bodies is essential for mitigating environmental contamination. (Ali et al., 2020)[5].

1.2.5 Expulsion of weighty metal particles from fluid arrangements

Weighty metal particles in water are not biodegradable and can cause cancer, leading to serious health issues for both aquatic life and humans who consume the contaminated water. To tackle this, various methods for eliminating weighty metal particles from water have been explored. Techniques such as electrocoagulation(EC), adsorption utilizing manufactured and normal adsorbents, utilization of attractive fields, high level oxidation processes, and membrane filtration have been studied. These studies have examined the benefits and burdens of each wastewater treatment method, specifically focusing on their effectiveness in removing heavy metals.

1.2.5.1 Methods utilized for evacuation of weighty metal particles:

1. Chemical precipitation: This method is the most widely used and efficient technique employed due to its low operational costs and simple procedures. In chemical precipitation, harmful metal ions react with compounds to form precipitates. These insoluble precipitates are then separated using two methods: filtration and sedimentation. Traditional precipitation consists of two main processes: sulfide chemical precipitation and hydrogen precipitation (Mishra et al., 2021)[47].

2. Ion exchange: This technique is commonly used to treat industrial wastewater due to its advantages, which include fast reaction rates, high treatment capacity, and excellent removal efficiency. This method is a reversible chemical process that can replace unwanted metal ions with environmentally friendly and safe ones. In this process a weighty metal particle is taken out from a wastewater arrangement by connecting it to a fixed strong molecule, replacing the particle's original cation. These strong particle trade particles can be produced using normal materials like inorganic zeolites or synthetic materials like organic resins (Vidu et al., 2020)(Qasem et al., 2021)[57][72].

3. Adsorption: The mechanism of adsorption depends on the physico chemical characteristics of the adsorbent and the weighty metals, as well as on factors such as temperature, adsorbent amount, pH level, adsorption time, and beginning metal particle focus. The adsorbent's surface can attract and hold heavy metal ions. This method is used extensively for its low working expenses, high evacuation proficiency, simplicity of execution, and direct treatment process (Qasem et al., 2021)[57]. It is also highly versatile, as adsorption can be reversed sometimes, allowing for the presence of various adsorbents to remove weighty metal particles. Moreover, the adsorbent can be reused during the desorption process (Mishra et al., 2021)[47]. Example: Activated carbon adsorbents, biosorbents, carbon nanotubes can be used as adsorbents.

4. Membrane filtration: Due to technological advancements in membrane development, membrane filtration and the extract of weighty metal particles from waste water have become more prevalent (Qasem et al., 2021)[57]. This method is highly effective, requires minimal space, and has a simple design. It is easy to use and offers high metal removal efficiency. Types of membrane filtration used are reverse osmosis,

electrodialysis, ultrafiltration, and nanofiltration (Vidu et al., 2020)(Mishra et al., 2021)[47][72].

Among various methods of heavy metal ions removal, adsorption technique is the most promising because its simple to use, have low cost and have high removal efficiency across wide range of pH.

1.3 PICKERING EMULGEL

1.3.1 General

Topical drug delivery systems have been used for centuries to treat local skin disorders and other targeted areas in the body. This localized approach involves applying a drug-containing formulation directly to the skin, eyes, rectum, or vagina, rather than administering the drug systemically. A skin drug conveyance framework is characterized as the utilization of a medication containing detailing to the skin or other accessible areas of the body to directly treat cutaneous (skin) or localized disorders. Topical drug delivery systems offer several advantages like localized treatment, reduced systemic exposure, improved patient compliance and avoidance of first pass metabolism (Mohite et al., 2019)[49].

1.3.2 Emulgel

Gels are new dosage forms that are used to deliver active pharmaceutical ingredient (API) to the site of action. Gels have three-dimensional and cross-linked structures to entrap small drug particles in network of colloidal solid particles and exhibit controlled release (Sriaandhal Sabalingam & Malitha Aravinda Siriwardhene, 2022)[63]. In comparison to ointments or creams, gels have a higher water content, which enhances drug solubility and facilitates easier drug migration. Gels have a significant drawback that they cannot effectively deliver hydrophobic medications. To overcome this limitation, emulgels are developed. Emulgels combine the benefits of gels, allowing even hydrophobic drugs to be effectively entrapped and released at the site of action (Vanpariya et al., 2021)[71].

1.3.2.1 Types of emulgel

1. **Macroemulgel:** These emulgels have particle sizes larger than 400 nm. Under a microscope, the droplets in macro-emulgels are visible and appear opaque and uniform.

2. **Nanoemulgel:** To create thermodynamically stable emulgels, nano-emulsions are added to gels. With droplet sizes smaller than 100 nm, nano-emulgels exhibit excellent penetration efficacy.
3. **Microemulgel:** These preparations form a thermodynamically stable formulation with particle sizes ranging from 10 to 100 nm. The formulation of micro-emulgels aids in the medication's penetration through the skin to reach the targeted location.

1.3.3 Pickering emulgel

Pickering emulsions are a type of emulsion stabilized by solid particulates instead of surfactants. S.U. Pickering, a British chemist gave the term pickering in 1907 (Chevalier & Bolzinger, 2013)[14]. Pickering emulsions due to their stability and encapsulation efficiency for both the hydrophobic and hydrophilic drugs have attracted keen interest in pharmaceutical sector. Another crucial aspect of Pickering emulsions is the formation of a thick shell surrounding the droplets by solid at the interface of oil and water, adsorbed particles. This shell functions as a physical barrier to prevent material transfer, which is advantageous for the controlled delivery of drugs. The improvement of a thick shell makes an actual hindrance that can stop chemicals from diffusing out of the capsule (Frelichowska et al., 2009)[33]. A Pickering emulsion forms a stabilising layer at the oil-water interface that prevents the two immiscible liquids from merging because of the adsorbed solid particles (Tang et al., 2014)[66]. The particles may be an organic compound, polymers, nanoparticles, clays or minerals. Pickering emulsions have a number of benefits over typical surfactant-stabilized emulsions, including better control over droplet size and shape, increased stability, and resistance to coalescence. They could be utilised in a variety of sectors, including the oil and gas industry, the cosmetics and pharmaceuticals sector, and the food and beverage sector (Dieng et al., 2020)[21].

Chemicals as well as biological agent exposure in a battlefield or in any industrial accident led to exposure of victims to hazardous substances. The contaminated person may be externally contaminated or internally depending on the route of administration, time of exposure and dosage of hazardous substance. It is observed over a time if exposure limit exceeds, external contamination may lead to internal contamination that may complicate the medical management of victims. Therefore, to prevent it,

decontamination is a necessary process of medical management of victims (Domínguez-Gadea & Cerezo, 2011)[22].

1.4 DECONTAMINATION OF SKIN

1.4.1 Skin

Skin is one of the biggest receptors in the human body that does several essential functions and acts as the first line of defence. It makes up about 10% of the total body mass and has an average area of 1.7 m². The skin can absorb topically applied ingredients, making it an increasingly most preferred route for delivering a variety of drug molecules (Ahmed et al., 2022)[3].

1.4.1.1 Design of skin

Skin is made out of three primary layers for example Epidermis, dermis and subcutaneous layer. The outermost layer is called the epidermis, below this dermis layer is present. Subcutaneous layer is made up of fatty cells and tissues.

- 1. Epidermis:** Epidermis is the peripheral layer of the skin that remaining parts in direct contact with the topically applied fixings and it is non-vascular in nature. Epidermis performs the barrier function and forms a protective covering made up of stratified squamous epithelium cells. Epidermis is partitioned into 5 layers for example Layer corneum, layer lucidum, layer granulosam, layer spinosum, and layer basale. Layer corneum is the outer most layers, which is the thickest layer (20-30 cells) while the stratum basale is the innermost layer.
- 2. Dermis:** The primary function of this layer is to support and give nourishment to epidermal cells physically. It consists of two layers: the reticular layer and the papillary layer. Both layers contain elastic fibers, fibrillin, and collagen. This layer also includes hair follicles, blood vessels, and nerve endings, as well as important glands like sweat and sebaceous glands. Also, it contains small blood vessels that provide the epidermis with nutrients, flexibility, and oxygen.
- 3. Subcutaneous layer:** It consists of fatty cells and tissues, which provides a cushion like protection to the body and performs the function of insulation (Ahmed et al., 2022)[3].

1.4.2 Decontamination

Decontamination refers to the process of reducing or removing chemical or biological agents to a level where they no longer pose a threat. These agents can be neutralized through physical or chemical means (detoxification).

1.4.2.1 Types of decontamination

Decontamination can be categorized into various types:

- a) **Personal decontamination:** Decontamination of an individual.
- b) **Casualty decontamination:** Decontamination of casualties.
- c) **Personnel decontamination:** Generally refers to decontamination of non-casualties. (Hurst, n.d.)[37]

1.4.2.2 Methods of decontamination:

- a) **Physical removal-** Significant amounts of chemical agents can be removed or diluted by flooding or flushing contaminated skin or materials with water or aqueous solutions. Using a wooden scraper stick, such as a Popsicle stick or tongue depressor, can physically remove bulk agents. The non-specificity of most physical methods is a major advantage.
- b) **Chemical removal-** Removing or reducing the threat from a contaminant involves making it less harmful through chemical changes such as oxidation, reduction, complexation, or chelation. These processes use reactive or catalytic chemicals, called sorbents, to neutralize the contaminants.
- c) **Biological removal-** Compared to chemical warfare attacks, decontaminating personnel and equipment after a biological warfare attack is generally less critical because most biological agents don't pose the same immediate threat. However, trichothecene mycotoxins are an exception, as they are not typical biological warfare agents. Despite this, decontamination remains an important method to prevent the spread of infections from potential aerosolization. Decontamination involves disinfecting or sterilizing contaminated items to make them safe for use, which means reducing microorganisms to an acceptable level. Contamination by biological agents refers to the introduction of microorganisms into tissues or sterile materials.

1.4.2.3 Selection of suitable decontaminant

When selecting the most suitable decontamination or cleanup methods, site-explicit variables should be thought of. These include: -Amount and form of the released chemical warfare agents (e.g., fume crest versus fluid beads)

- Weather conditions (temperature, humidity, etc.)
- Types of surfaces needing decontamination: non-porous surfaces, permeable surfaces like soil, cement, or black-top, metal surfaces, hardware, or human skin
- The size and intricacy of the impacted region
- Possible future purposes of the area
- Anticipated human openness
- Availability of resources. (Talmage et al., 2007)[65]

Chemical warfare agents that can damage the skin or penetrate it to cause systemic poisoning primarily target the external environment (Karakurt & Başı, 2024)[43]. Exposure to chemical weapons allows harmful toxins to enter the human body through various systems. For instance, chemical weapons in liquid and solid forms can be absorbed through the skin and then enter the body. In contrast, gas and vapor forms are primarily inhaled through the respiratory system, subsequently entering the circulatory system. Skin infections caused by chemical warfare agents pose a significant threat to both military and civilian populations during modern conflicts or terrorist acts. These agents can cause unconsciousness, respiratory depression, anxiety, increased heart rate, hypertension, and muscle paralysis. To reduce toxicity, it is crucial to remove any CBRN (substance, natural, radiological, and atomic) agents from the skin as quickly as possible. Effective decontamination also extends the time available for treatment (Karakurt & Başı, 2024)[43].

1.4.2.4 Commercially available formulations for decontamination:

- **Sandia Froth**, created by Sandia Public Research facility and mentioned by the U.S. EPA, contains surfactants and oxidizers like hydrogen peroxide (H₂O₂) in various combinations. Though it starts as a fluid, it tends to be applied as a spray, fluid, or froth, contingent upon the application instrument. Tests show its viability against both compound and natural specialists, primarily due to action of H₂O₂.

- **RSDL (Receptive Skin Disinfecting Moisturizer)**, a fresher item was created by the Canadian Guard Exploration Foundation. RSDL is a yellow, gooey fluid impregnated into a wipe cushion and put away in a foil pocket. It is known for its broad-spectrum decontaminant properties, minimal irritation, and easy removal with water. After testing by Battelle's Clinical Exploration and Assessment Office in Columbus, Ohio, the U.S. Food and Medication Organization supported RSDL for application in 2003.

CHAPTER-2
REVIEW OF LITERATURE

CHAPTER-2

REVIEW OF LITERATURE

1. Bas *et al.* 2024, Pollutants classified as synthetic, organic, radiological, and atomic (CBRN) present dangers to general wellbeing, the environment, property, and population safety. Decontamination is a crucial step in CBRN incidents. It involves removing or reducing chemical, biological, radiological, and nuclear contaminants from people, vehicles, materials, buildings, and other areas to levels that do not pose a threat to human health. Effective decontamination is essential in combating CBRN warfare agents. It involves physically removing or chemically neutralizing the agents, which helps clean individuals exposed to these hazards. Studies suggest that 90% of contamination can be removed within one minute if skin decontamination and clothing removal are performed promptly.

2. Geng *et al.* 2024, A review was led to assess the use of defatted grape seed powder (DGSP) as a stabilizer for Pickering emulsion gels, potentially replacing butter. The DGSP was utilized to form the emulsion gel through high-speed homogenization. The results revealed a three-phase contact angle of $128.9 \pm 2.3^\circ$, a broad range of particle sizes (3–130 μm), and diverse particle shapes in the DGSP. When the particle concentration was at least 2% ($c \geq 2\%$), and the oil-phase volume fraction was 60% or higher ($\phi \geq 60\%$), stable O/W Pickering emulsion gels could be formed. The gel strength increased with both higher particle concentration and oil-phase volume fraction. Conversely, the droplet diameter decreased with higher particle concentration and increased with higher oil-phase volume fraction. The resulting emulsion gel exhibited viscoelastic behavior similar to that of a solid.

3. Budi *et al.* 2024, Heavy metals, toxic even at low concentrations, pose significant health risks due to agricultural and industrial activities, improper waste disposal, and wastewater discharge. A narrative review from 2000 to 2022 across databases like Google Scholar and PubMed identified 820 articles, with 45 selected for analysis. These studies reveal that the adverse effects of heavy metals rely upon elements, for

example, dose, exposure route, and individual characteristics. Long-term and short-term exposure to heavy metals is linked to various health issues, including carcinogenicity. However, the mechanisms remain unclear, highlighting the need for comprehensive research on heavy metals' carcinogenic effects.

4. Wang *et al.* 2024, This study explores the effectiveness of Ca²⁺-actuated persistent stage gelation of ovalbumin(OVA)- low meth oxyl gelatin(LMP) electrostatic complex particles(OLECP) in settling high inside stage Pickering emulsions(HIPPEs).The research compares HIPPEs and HIPPEs gel across various LMP concentrations, revealing that continuous phase gelation enhances viscoelasticity, water binding, and hardness. Observations show a robust network structure in HIPPEs gel, with finer 3D gel networks and smaller oil droplet sizes at higher pectin concentrations. Encapsulation in HIPPEs gel improves curcumin's photochemical stability and bioaccessibility, and promotes fat hydrolysis. However, HIPPEs gel exhibits poor printability compared to HIPPEs.

5. Pang *et al.* 2023, The nonstop release of effluents containing weighty metals from tanneries, mining, printing, and drug businesses into oceanic conditions has turned into a difficult issue. Chromium (Cr) and mercury (Hg) are especially perilous to human wellbeing. Different strategies have been utilized to resolve this issue, including adsorption, electrolysis, compound precipitation, desalination, switch assimilation, particle trade, film filtration, and photocatalysis. Among these, photocatalysis stands apart for its expense adequacy and harmless to the ecosystem way to deal with eliminating weighty metal particles from arrangements.

6. Xu *et al.* 2023, Since the atomic bomb assaults on Hiroshima & Nagasaki in 1945,advancements in nuclear technology have been significant. In modern times, nuclear bombs could target larger areas, cover longer distances, and exhibit much greater destructive force. This has led to growing concerns about the potentially catastrophic humanitarian consequences. The discussion encompassed the actual conditions created by a nuclear bomb detonation, including radiation injuries and diseases. Additionally, the analysis addressed worries about the usefulness of clinical consideration frameworks and their supporting foundation — like transportation,

energy, and supply chains — following a gigantic atomic assault. Whether or not residents could make due such an event was also examined.

7. Cauweret et al. 2023, This study aimed to identify and analyze all reported terrorist attacks on nuclear transport, facilities, and scientists over the past 50 years, as documented in the Global Terrorism Database (GTD). The GTD was examined for terrorist attacks targeting nuclear facilities, scientists, transport, and other industry-related sites from 1970 to 2020. The data was analyzed based on the timing, location, target type, method and weapon used, type of perpetrator, number of casualties, and property damage. From 1970 to 2020, 91 incidents were recorded. These incidents occurred in 25 countries across nine regions, with the highest number (42 incidents, 46.1%) happening in Western Europe. In these 50 years, the 91 incidents led to 19 deaths and 117 injuries. One perpetrator was killed, and another was injured during these incidents.

8. Shukla et al. 2023, Metal pollution from military operations has been linked to environmental contamination and health risks. This essay examines how military activities release metals such as lead(Pb), copper(Cu), cadmium(Cd), antimony(Sb), chromium(Cr), nickel(Ni),also, zinc(Zn) into the climate. Gun shot residue(GSR) can cause significant metal pollution in both indoor and outdoor settings. People are exposed to these metals through ingestion, inhalation, and injuries involving metal fragments. Research indicates that military personnel exposed to these metals may suffer from neurological, cardiovascular, and reproductive issues. Residents near contaminated areas may experience respiratory, visual, and neurodevelopmental problems. Metal pollution also affects animals, plants, soil, and water sources.

9. Abdel-Raouf et al. 2022, Study shows that depending on the pH level, the biosorbents *Phormidium tenue* and *Chlorella vulgaris* have different capacity for absorbing Co^{2+} , with greater efficacy at optimum pH values. The study investigates potential utilization of *Chlorella vulgaris* and *Phormidium tenue* as absorbents for the bio removal of Co^{2+} metal from fluid arrangements. The results of the study can help develop effective bioremoval techniques for heavy metal pollutants in environmental remediation applications.

10. Skalny *et al.* 2021, This research suggests that military operations and armed conflicts contribute to environmental metal contamination. Key sources include weapon residues containing lead (Pb), copper (Cu), and depleted uranium (DU), which release metals into the environment during military actions. This contamination increases human exposure risks through soil and water pollution with metals such as Cd, Sb, Cr, Ni, and Zn. Biomonitoring studies indicate higher metal accumulation in plants, invertebrates, and vertebrates. Military activities are linked to metal exposure through ingestion, inhalation, and injuries from embedded metal shards. Exposed military personnel suffer neurological, cardiovascular, and reproductive issues, while children in contaminated areas face neurodevelopmental problems.

11. Qasem *et al.* 2021, This review evaluates methods for removing heavy metal particles from wastewater, including adsorption, ion exchange, membrane, electric, and photocatalytic treatments. Key findings highlight a focus on adsorption techniques, which face challenges such as concurrent ion removal, retention time, and cycling stability. Chemical and membrane methods encounter issues with sludge formation and post-treatment requirements, while membrane methods also suffer from fouling and scaling. Electrical methods require industrial-scale application and address sludge formation. Future research should prioritize eco-friendly, cost-effective, and sustainable approaches, using real wastewater samples.

12. Charles *et al.* 2020, This review paper discusses advancements in scientific methods used to analyze gunshot residues, as reported after the 17th Interpol Forensic Science Symposium in October 2016. A literature review was conducted, focusing on publications from major forensic and analytical journals from 2016, 2017, and 2018. When a firearm is discharged, it releases primer and gunpowder residues, metal fragments from the projectile and cartridge case, and other debris from the muzzle and other gun openings. These residues are collectively referred to as gunshot residues (GSR), firearm discharge residues, or primer residues.

13. Ali *et al.* 2020, This study demonstrated the effective removal of strontium using the cost-effective Dowex-HCR-S/S (DHS) resin. Using the batch method, the sorption properties showed that the pseudo-second-order dynamic model fit well & the sorption isotherm models indicated an equilibrium monolayer capacity of 400.0 mg/g for Sr(II).

Thermodynamic parameters confirmed that the expulsion cycle was unconstrained and endothermic. DHS resin effectively removed ^{85}Sr from organic liquid scintillator waste and various environmental waters, including tap, river, seawater, and groundwater. The study concludes that DHS resin is a highly effective, low-cost option for removing ^{90}Sr from radioactive wastewater and environmental sources.

14. Mishra *et al.* 2020, Heavy metals in wastewater are a major contributor to environmental pollution, affecting the soil where we grow crops, the air we breathe, and the water we drink. These metal ions pose a significant environmental challenge today. To address this issue, various methods have been employed to manage metal ions. This review has explored several techniques, including ion-exchange, chemical precipitation, flotation, adsorption, membrane filtration, electrochemical methods, and coagulation-flocculation. Research and literature reviews indicate that the most commonly used methods for removing metal ions from wastewater effluent are membrane filtration, ion-exchange, and adsorption.

15. Vidu *et al.* 2020, This review summarizes the ongoing challenge of removing heavy metals from wastewater, given that they are key contaminants that do not biodegrade and instead accumulate in the ecosystem. Their persistent nature, toxicity, and accumulation in the human body necessitate the development of new and more effective water treatment methods to reduce heavy metal concentrations. Nanotechnology presents several advantages over other techniques, such as volumetric efficiency and more effective and faster processes at the nanoscale. This review provides an updated report on the primary technologies and materials used for heavy metal removal, with a focus on nanoscale materials and processes, considering the multidisciplinary research involved in water treatment.

16. Tomonaga *et al.* 2019, Seventy-four years ago the nuclear bombings of Hiroshima and Nagasaki, killed around 210,000 casualties and left another 210,000 as survivors. The wellbeing impacts on these survivors, known as hibakusha, have persisted through three phases: the emergence of leukemia in 1949, the development of various cancers in the intermediate phase, and a lifelong battle with cancers for those who were children at the time of the bombings. Elderly hibakusha have also experienced a second wave of leukemia and suffer from psychological issues such as depression and PTSD. As a

result, the human toll of these bombings is ongoing, with many still dying from radiation-induced illnesses. Hibakusha have continuously fought to rebuild their lives under the shadow of disease and have led a movement to eliminate nuclear weapons.

17. Gruss *et al.* 2019, This research investigated soil pollution at military sites in Ukraine brought about by titanium (Ti) and iron (Fe) utilizing aversion and propagation tests with *Folsomia candida* (springtails). Soil samples from polluted and control sites in Dolyna, Ivano-Frankivsk, revealed higher Ti and Fe levels at the control site. Nine contamination levels (1%-100%) were tested. The seven-day avoidance test and twenty-eight-day reproduction test showed significant reductions in *F. candida* presence at concentrations of 1.5%-100%, with no avoidance at 1%. Reproduction was negatively affected at 10%, with EC50 values of 50.12% for avoidance and 22.39% for reproduction, indicating heavy metal toxicity at military sites.

18. Xing *et al.* 2019, Graphene oxide(GO) was synthesized, characterizes, utilized to adsorb Sr (II) from an aqueous solution. According to the Langmuir model, the adsorption limit was determined to be 137.80 mg/ g. The crystal structure of the Sr compound on graphene sheets was examined using scanning electron microscopy with an energy dispersive X-beam locator(SEM-EDX), high-resolution transmission electron microscopy(HRTEM), and X-beam diffraction(XRD). Fourier transform infrared spectroscopy(FTIR) and X beam photoelectron spectroscopy(XPS) examinations uncovered the association of O-C=O, C-O, and C-O-C groupings in the adsorption interaction.

19. Curling *et al.* 2016, This study developed a methodology to evaluate the credibility of radiological materials as threats by comparing the amount typically found in commercial practice ("P") with the quantity necessary to pose a significant threat ("C"). A high P/C ratio (≥ 0.1) indicates a more credible threat. The study assessed various dispersal mechanisms and scenarios, focusing on an acute radiation dose of 1.25 Sv. Radioisotopes such as ^{60}Co , ^{75}Se , ^{90}Sr , ^{137}Cs , and others were evaluated for their potential use in radiological dispersal devices (RDDs). The analysis concluded that radiological weapons, despite technological challenges, pose credible threats to military operations due to the availability of radioactive materials in commercial sectors. RDDs are primarily intended to induce fear and disrupt, termed "weapons of mass disruption."

20. Czarnek *et al.* 2015, This review paper discussed the activity of cobalt particles in the human's body. The body can absorb cobalt through food, inhalation, skin contact, and as a part of biomaterials. For nearly 40 years, cobalt and its alloys have been vital in orthopedic implants. Toxic inorganic cobalt can accumulate in tissues, causing cellular changes. The release of cobalt ions from implant surfaces can trigger harmful and immune responses. Long-term cobalt ion release can lead to metallosis due to high cobalt levels. These ions can also accumulate in organs like the kidneys, liver, spleen, heart, and lymph nodes, and are excreted through waste and urine. Cobalt ions may cause genotoxicity and cytotoxicity in cells.

21. Tayyebi *et al.* 2015, The synthesis of magnetite nanoparticles (M) and their integration onto graphene oxide (GO) via ultrasound-assisted precipitation advances nanomaterial fabrication. This yields M-GO hybrids with finer size distributions and a saturation magnetization of 31 emu g^{-1} . The Langevin equation estimates Fe_3O_4 nanoparticle sizes within the M-GO hybrid with 17.5% maximum error. Instrumental analyses were employed to clarify the mechanisms of formation. Adsorption studies of Sr^{+2} and Co^{+2} ions on M-GO showed that the Langmuir monolayer model fits well, indicating that Co^{+2} ions exhibit higher adsorption capacities similar to Fe^{+2} in Fe_3O_4 . Endothermic and spontaneous ion uptake occurs through different mechanisms: inner-shell complex formation for Co^{+2} and ion exchange for Sr^{+2} . Enhanced ion sorption above pH 5 highlights the role of surface charge and deprotonation reactions.

22. Jaishankar *et al.* 2014, Heavy metal toxicity poses a significant health threat, with various metals showing toxic effects that harm human health and disrupt normal bodily functions. These metals, despite having no biological purpose, can sometimes act as false components in the body, leading to metabolic issues. To address metal toxicity from sources like work related openness, mishaps, and natural factors, various general wellbeing drives have been sent off. The poisonousness of metals relies upon the retained portion, openness route, and whether the exposure is acute or chronic. This can result in oxidative stress caused by free radicals, leading to numerous illnesses and extensive damage. This review explores the health impacts and toxicity mechanisms of several heavy metals.

23. Chevalier *et al.* 2013, Pickering emulsions are attractive formulations due to their simplicity and similarity to traditional surfactant-based emulsions. Despite being discovered in 1907, they received little attention until a renewed interest emerged recently. The main objective of this review is to introduce beginners to the topic by explaining the basic principles. The review covers the fundamental physical chemistry of Pickering emulsions and methods for controlling key variables important for application development. The first section discusses the selection and surface properties of solid nanoparticles used as stabilizers, as well as the emulsion type, droplet size, and rheology.

24. Simonsen *et al.* 2012, This review explores cobalt's metabolism and toxicity. While cobalt is vital for health, excessive amounts are toxic. It interferes with oxygen sensing in cells and can cause cytotoxicity, apoptosis, necrosis, and inflammation at high doses. Cobalt's genotoxicity is linked to oxidative DNA damage and impaired DNA repair. Animal studies confirm its carcinogenicity, but human data are insufficient. Cobalt inhibits calcium signaling and accumulates in the liver, kidneys, pancreas, and heart. Occupational exposure, especially in cobalt processing and hard-metal industries, has decreased with better hygiene practices, though adverse effects at current exposure limits still occur.

25. Chowdhury *et al.* 2011, Among the alkaline earth metals, strontium (Sr) shares characteristics with calcium (Ca). Environmental strontium is considered hazardous, and it is not required by humans or other species due to the radioactive risks posed by its radionuclides. This study summarizes physiological and toxicological data relevant to stable and radioactive Sr in fish inhabiting freshwater and marine environments. The chemistry, bioaccumulation, and toxic effects are briefly discussed before delving into the mechanisms of Sr absorption, internal processing, and excretion in fish.

26. Frelichowska *et al.* 2009, The study investigated the permeation of caffeine using a water-in-oil (w/o) Pickering emulsion (PE) in contrast to a conventional emulsion balanced out utilizing an emulsifier. The two emulsions had indistinguishable syntheses and physicochemical properties. The Pickering emulsion showed a higher saturation rate, with a pseudo consistent state transition of $25\text{gcm}^{-2}\text{h}^{-1}$, three times that of the classical emulsion. After 24 hours, caffeine was primarily found in the dermis and

receptor fluid, with higher cumulative levels in the Pickering emulsion. Enhanced penetration was attributed to better adherence of Pickering emulsion droplets to the skin and significant penetration of silica particle aggregates into the stratum corneum.

27. Barnaby 2005, A radiological weapon is the simplest and most primitive form of a terrorist nuclear device. A dirty bomb combines conventional explosives with radioactive materials like cesium-137. There are a huge number of radioactive sources utilized worldwide in medication, industry, and horticulture, many of which could be repurposed to create a dirty bomb. These sources are often not securely stored, making it feasible for terrorists to obtain radioactive material. The immediate casualties and injuries from the blast and long-term cancers due to radiation exposure would likely be minimal. However, the real impact of a dirty bomb lies in the massive social, psychological, and economic disruption caused by radioactive contamination. The explosion of a dirty bomb could contaminate tens of square kilometers in a city, necessitating evacuation and extensive decontamination.

28. Jarupet al. 2003, Heavy metals like Pb, cadmium, Hg, and Ar present critical wellbeing gambles. Despite known adverse effects, exposure persists, especially in less developed countries, though it has declined in developed nations. Cadmium, used in batteries, has seen increased emissions due to poor recycling practices. Major sources of exposure are smoking and food, causing kidney damage and bone issues even at low levels. Mercury exposure mainly comes from fish and dental amalgams. While general risk is low, pregnant women should avoid high-mercury fish to prevent neurological damage to fetuses. Lead exposure, from air and food, remains a concern, especially for children, due to neurotoxic effects at low levels. Arsenic exposure through food and water increases risks of skin and lung cancer.

29. Barceloux et al. 1999, This review explores cobalt's presence in nature, industrial applications, health impacts, and associated toxicities. Found primarily as arsenides, oxides, and sulfides, cobalt's industrial use in metallic form is pivotal, notably in cobalt superalloys and "hard metals" alongside tungsten carbide and nickel. While dietary intake is common, occupational exposure, especially in cobalt powder production, poses risks, often coupled with tungsten in hard metal fabrication. Crucial for vitamin B12 synthesis, cobalt's delicate balance between sufficiency and excess underscores its

dual health impact. Excessive intake can lead to goiter and thyroid dysfunction. Dermatological conditions and respiratory afflictions, such as allergic contact dermatitis and occupational asthma, are also linked to cobalt exposure. Management of cobalt toxicity focuses on supportive measures to alleviate symptoms and prevent further exposure.

CHAPTER-3
AIM AND OBJECTIVES

CHAPTER-3

AIM AND OBJECTIVES

3.1 AIM:

Decontamination efficacy of graphene oxide and silanized graphene oxide based Pickering emulsions for removal of heavy metal ions.

3.2 OBJECTIVES:

1. Synthesis of silanized graphene oxide (sGO)
2. Characterization of synthesized sGO
3. Adsorptive expulsion of heavy metal particles from watery arrangement by AAS and complexation analysis by fluorescence spectroscopy
4. Synthesis and characterization of Pickering emulsion
5. Decontamination studies

3.3 PLAN OF WORK

- 1] Survey of Writing
- 2] Choice of medication and excipients
- 3] Acquisition of medication and chemicals
- 4] Synthesis of sGO from GO
- 5] Characterization of GO and sGO
 - Fourier transform infrared spectroscopy (FTIR)
 - Thermogravimetric analysis (TGA), FE-SEM
 - Raman spectroscopy
- 6] Adsorptive expulsion of heavy metal particles from watery arrangement by AAS and complexation analysis by fluorescence spectroscopy
 - By AAS: Effect of dose and effect of contact time
- 7] Synthesis of formulation
 - Preparation of Pickering emulsion
- 8] Characterization of formulation
 - Physical appearance

- pH Determination
- Particle Size Analysis
- Zeta Potential
- Optical microscopy
- Rheological studies
- Differential scanning calorimetry (DSC)
- FT-IR
- Contact angle
- FE-SEM
- Stability studies

9] Decontamination studies

10] Thesis writing and compilation

3.4 RATIONALE

We are targeting decontamination of skin from heavy metal ions using GO and sGO based Pickering emulgels. Contamination of skin when it comes in contact with heavy metal ions is a great concern for army or military personnels and individuals residing in that particular area. Skin is the primary and largest organ that comes in contact with the heavy metal ions and pose risks for contamination. Heavy metal ions on contact with skin penetrates inside and cause several toxicities. They also cause several allergies on skin causing irritation. The objective of this research work is to minimize the contact time of heavy metal ions with the skin to prevent their penetration and hence prevent the toxicity. Emulgels have three-dimensional and cross-linked structures to entrap small drug particles in network of colloidal solid particles and exhibit controlled release. Emulgels deliver the drug to specific site and are non-sticky, non-greasy preparations so they are prevalent dosage form nowadays. In comparison to ointments or creams, gels have a higher water content, which enhances drug solubility and facilitates easier drug migration that's why we are preferring this dosage form. Pickering emulgels are formulations stabilized by solid particles that are irreversibly adsorbed on the interface. GO and sGO are powerful drug substance that remain in solid state. So, PE formulation will be suitable approach for GO and sGO.

CHAPTER-4
DRUG PROFILE

CHAPTER-4

DRUG PROFILE

4.1 Drug's Profile

4.1.1 Graphene Oxide

Structure:

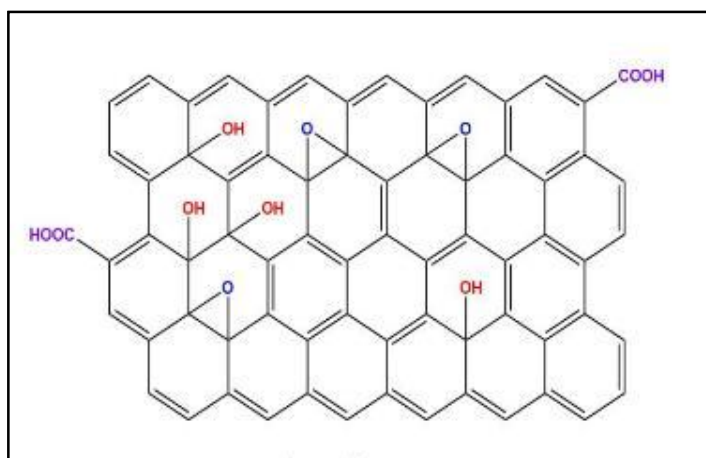


Fig 4.1: Structure of Graphene oxide

- Graphene oxide (GO), a layered carbon structure, highlights oxygen-containing useful gatherings (=O, - Gracious, - O-, - COOH) joined to both the edges and surfaces of its layers.
- GO exists as a monolayer sheet with hydroxyl, carboxyl, and epoxy oxygen bunches present on its edges and basal plane, leading to a combination of sp² and sp³ hybridized carbon atoms.
- GO finds application in advanced fields like drug delivery, high-temperature materials, and construction materials.(Jiříčková et al., 2022)[41].

4.1.2 Silanized Graphene Oxide

Silanized graphene oxide is a silane functionalized GO synthesized using APTES as the silane precursor. Its properties are similar to GO.

Structure:

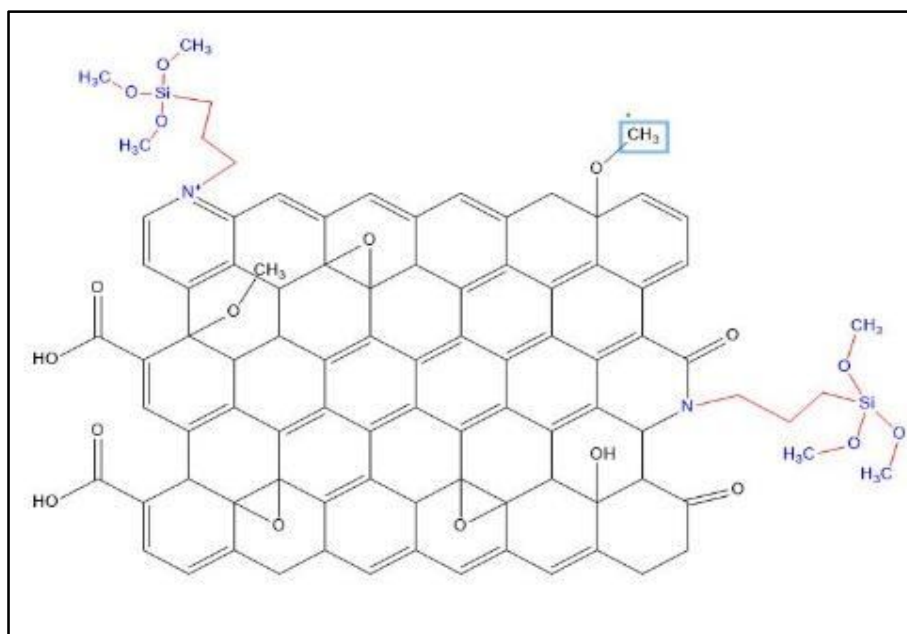


Fig 4.2: Structure of Silanized Graphene Oxide

4.2 Excipients Profile(Goel et al., 2023)[34]

4.2.1 Diethyl adipate

Diethyl adipate is a fatty acid ethyl ester and it is a colorless liquid. It is formed by esterification of adipic acid with ethyl alcohol.

Structure:

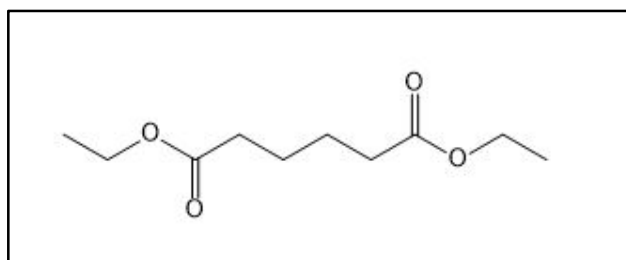


Fig 4.3: Structure of diethyl adipate

Molecular formula:C₁₀H₁₈O₄

Atomic wt.: 202.25 g/mol

IUPAC' name: Diethyl hexanedioate

B.P.: 245 ° C

Liquefying Point: -19.8 ° C

Dissolvability: Solvent in ethanol and ethyl ester

4.2.2 *Kolliphorel*

It is pale yellow oily liquid which appears clear above 26°C and have faint characteristic odour.

Structure:

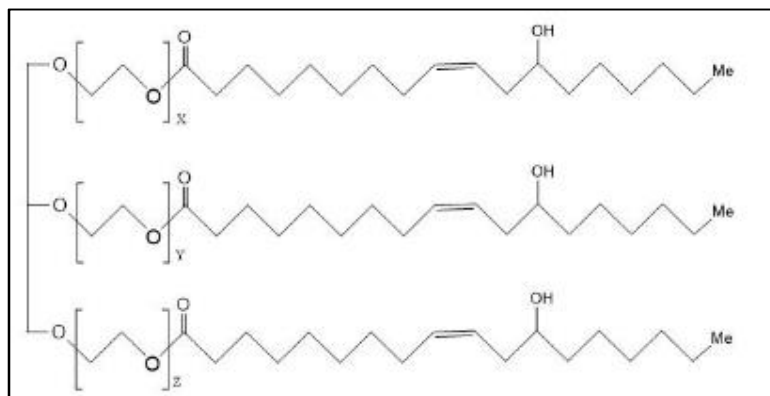


Fig 4.4: Structure of Kolliphorel

Chemical Name: Polyethoxylated castor oil

Melting Point: 19-20°C

HLB value: 12-14 (Emulsifying agent)

pH: 6-8

Solubility: Soluble in water, castor oil, chloroform, ethanol

4.2.3 *Xanthum gum*

It is a high sub-atomic weight polysaccharide gum having gelling, viscosity increasing and stabilizing properties.

Structure:

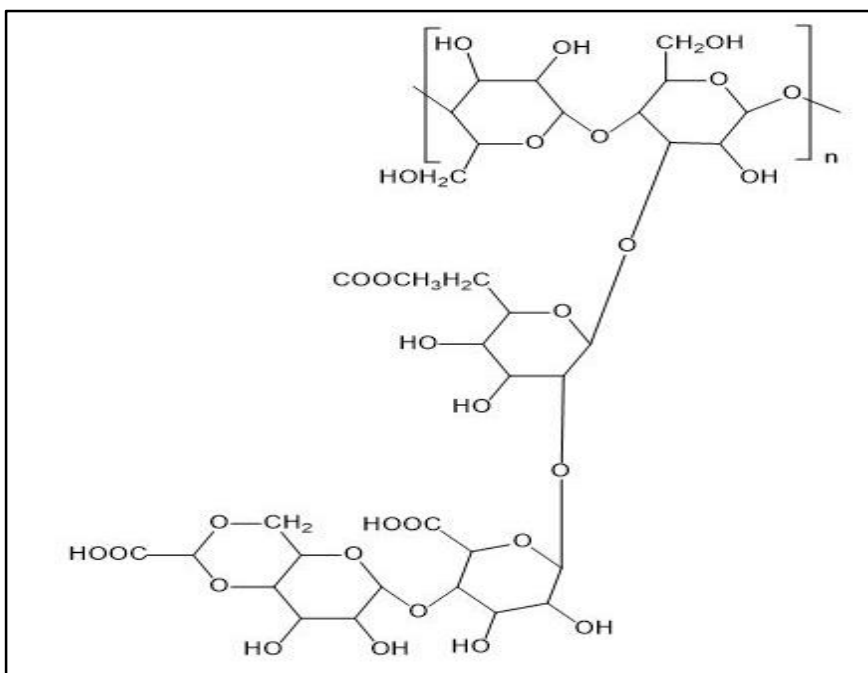


Fig 4.5: Structure of Xanthum gum

Molecular Formula: $(C_{35}H_{49}O_{29})_n$

Melting Point: Chars at 270°C

pH: 6-8

Solubility: Practically insoluble in ethanol and ether; soluble in cold or warmwater.

4.2.4 Glycerol

Glycerol is a transparent, colourless, odourless, thick liquid that takes moisture from the air. It is about 60% as sweet as sucrose.

Structure:

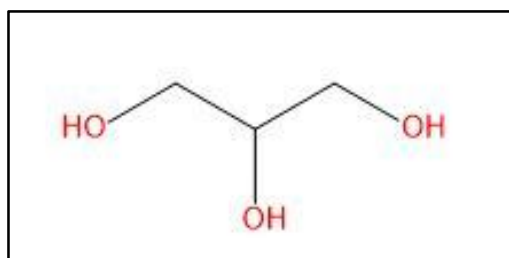


Fig 4.6: Structure of glycerol

Molecular formula: C₃H₈O₃

Molecular weight:96.02

Chemical name: Propane-1,2,3-triol

Edge of boiling over: 290°C

Melting Point: 17.8°C

Solubility: Dissolvable in water and methanol, basically insoluble in benzene &chloroform.

CHAPTER-5
INSTRUMENTATION,
MATERIALS AND
METHODOLOGY

CHAPTER-5

INSTRUMENTATION, MATERIALS AND METHODOLOGY

5.1 Instrumentation

5.1.1 Fluorescence spectroscopy



Fig 5.1: Fluorescence spectrometer

Fluorescence spectroscopy is a quick and sensitive technique used to analyze the molecular surroundings and processes within samples. Fluorimetry is preferred method because of its outstanding sensitivity, precise specificity, ease of use, and cost-effectiveness in contrast to other analytical methods. This widely acknowledged method finds application in forensics, genetic analysis, medical diagnostics, industrial processes, environmental monitoring, and biotechnology. It serves as an invaluable apparatus for both quantitative and subjective investigation. (Prasad & Krishna, n.d.) [55].

- ❖ **Principle:** When molecules absorb UV or noticeable radiation, their electrons move from the singlet ground state to the singlet invigorated state. Because the excited state is unstable, the molecules release energy as they return to the singlet ground state, emitting UV or apparent radiation all the while. Fluorescence discharge happens when the fluorophore changes from its singlet electronic energized state to a particular vibrational level in the electronic ground state, emitting detectable signals that can be measured and analyzed.

❖ **Instrumentation:**

A. Source of light: Lamp generates a wide range of visible and ultraviolet light.

Example: Mercury fume light, Xenon circular segment light, Tungsten film.

B. Channels and Monochromators:

Two types of Channels/monochromators are used to convert polychromatic light into monochromatic light.

a) Primary filter/ Excitation monochromator - Allows UV radiation to pass through and absorbs visible radiation for excitation.

b) Secondary filter/ Emission monochromator - Allows fluorescence radiation to pass through and absorbs UV radiation for emission.

C. Sample cells: Quartz cells are used, transparent from all sides.

D. Detectors: The emitted fluorescent radiation is measured by the detectors example:

Photomultiplier tube.

❖ **Working:** Light emitted from the xenon lamp reaches the entry cut of excitation monochromator. The excitation monochromator allows to pass a selected wavelength of light that strikes the example. Some amount of light is consumed by the example, causing some molecules to fluoresce. The emitted light is then directed into the emanation monochromator, which is situated at a 90° point to the excitation light way to limit the gamble of communicated or mirrored excitation light arriving at the finder. The emitted light passes through a restricted reach fixated on the predefined emanation frequency and ways out through customizable cuts, ultimately arriving at the indicator. The sign is enhanced, making a voltage that relates to the deliberate discharged power (Naresh, n.d.)[51].

❖ **Applications:** Examination of compound designs and cycles, Chemical analysis (Detection of impurity, Estimation of fluorescent intensity), Laser incited fluorescence spectroscopy of human tissues for disease finding, Investigation of marine petrol contaminations, An exceptionally delicate fluorescent immunoassay in view of avidin marked nanocrystals (Bose et.al., 2018)[12].

5.1.2 Fourier Change Infrared Spectroscopy (FTIR)



Fig 5.2: Fourier Change Infrared Spectrometer'

Fourier transform infrared (FTIR) spectroscopy is a highly effective spectroscopic technique for detecting functional groups in any compounds and identifying conceivable sub-atomic connections between synthetic mixtures. Distinguishing the spot of IR assimilation groups in the range, estimated in wave number, can assist with recognizing different substance parts (e.g., sweet-smelling amides) that probably won't be apparent with X-beam photoelectron spectroscopy. IR spectroscopy is widely applicable to many materials and used for both qualitative and quantitative analysis (Mohamed et al., 2017)[48].

FTIR spectroscopic analysis is advantageous over dispersive or channel strategies for IR ghastly investigation on the grounds that of:

- i.** It is a procedure wherein test is not destroyed (nondestructive).
- ii.** It gives an accurate estimation strategy that don't requires outer adjustment.
- iii.** It has good optical efficiency.
- iv.** It has only one moving part and hence mechanically simple.
- v.** It can improve speed, gathering an output consistently.
- vi.** It can improve awareness as it can examine consistently and these can be added together to proportion out irregular commotion (Dutta, 2017)[25].

- ❖ **Principle:** Assimilation of electromagnetic radiation in the infrared area of the range causes changes among rotational and vibrational energy levels inside the ground electronic state. (Berthomieu and Hienerwadel, 2009)[10]. The infrared (IR) district is by and large separated into three subregions: close IR (14,000-4,000 cm^{-1}), mid-IR (4,000-400 cm^{-1}), and far-IR (400-10 cm^{-1}). IR photons have sufficient energy to cause sub-atomic vibrations, making gatherings of molecules move comparative with their bonds. These vibrational changes happen at explicit energies, so particles ingest IR radiation at specific frequencies and frequencies. Synthetic bonds have trademark vibrational frequencies and assimilate IR radiation at frequencies that match their vibrational modes. By estimating these retention frequencies, a range is delivered, which can be utilized to distinguish useful gatherings and mixtures. Impurities also show unique bands in the IR spectrum, allowing for the determination of their concentrations and interactions with the host material. (Dutta, 2017)[25].
- ❖ **Instrumentation:** FT infrared spectrometer comprises three main components: a radiation source, an interferometer, and an indicator. The interferometer divides the brilliant shafts, makes an optical way distinction among them, and produces obstruction flags that the finder estimates in light of this optical way contrast. The interferometer produces impedance signals containing IR ghashly data subsequent to going through the example. The most usually utilized interferometer is the Michelson interferometer which has three key parts: a moving mirror, a proper mirror, and a pillar splitter. The two mirrors are organized opposite to one another. The pillar splitter, commonly made by saving a slim germanium film onto a level potassium bromide (KBr) substrate, is a semi-intelligent gadget. Radiation from the broadband IR source is collimated and coordinated into the interferometer, where it strikes the pillar splitter.
- ❖ **Working:** In an IR spectroscopy assembly, infrared energy is transmitted from a warmed blackbody source that goes through a gap, controlling how much energy coordinated onto the example (Griffith, 1983). Consequently, the pillar enters the interferometer, where ghashly encoding happens. The subsequent interferogram signal leaves the interferometer. On leaving the interferometer, the shaft enters the example compartment and either transmits through or reflecting off the sample's surface. At this stage, the infrared energy, consisting

specific frequency unique to the sample, is absorbed. Following this, the beam proceeds to the detector where it undergoes last estimation. The identifiers are designed to catch the extraordinary interferogram signal. The recognized sign goes through digitization before transmission to the PC for Fourier change. Thusly, the Fourier change process produces the infrared range, addressing power versus recurrence, which is then given to the client to investigation and understanding (Mohamed et al., 2017)(Dutta, 2017)[25][48].

❖ **Applications:**

- a) Examination of nanomaterials
 - b) Analysis of food including added substances, additives, and colorants
 - c) Environmental evaluation including water investigation, gases examination
 - d) Forensic examinations: paints, materials, and beauty care products
 - e) Pharmaceuticals investigation
 - f) Analysis of physiological examples like dangerous cells, bones, and hairs
 - g) Assessment of multi-facet intensifies like polymers, canvases, and movies
- (Dutta, 2017)[25]

5.1.3 Atomic Absorption Spectroscopy



Fig 5.3: Atomic Absorption Spectrophotometer

AAS, or nuclear retention spectroscopy, is a logical strategy that actions the convergence of metal molecules or particles that are available in an example. Around 75% of the substance components found on Earth are metals (Platt, 1971)(Bings et al., 2008)[11][54]. In environmental monitoring, AAS is often employed to analyze samples of air, water, soil, and sediment for trace metals. Clinical laboratories utilize

AAS for assessing metal ions in biological samples such serum, urine, and blood[11]. It is employed to measure the metal impurity concentration and guarantee adherence to legal requirements. It is used for assessing the concentrations of metals in raw materials, intermediate products, and final products in sectors like metallurgy, chemical manufacture, and electroplating(Robinson, n.d.)

❖ **Principle:** Each and every atom and ion can absorb light of specific and unique wavelengths. Electrons in an atom exhibit different energy levels. At the point when particles are presented to their trademark frequency, it ingests energy making electrons move to invigorated state from ground state. The energy which is consumed by the electrons is straightforwardly relative to the changes that happen in the electrons. Since every component has an unmistakable electronic construction, the consumed radiation is one of a kind. When atoms are exposed to their characteristic wavelength, it absorbs energy causing electrons to move to excited state from ground state. The energy which is absorbed by the electrons is directly proportional to the transitions that occur in the electrons. Since each element has a distinct electronic structure, the absorbed radiation is unique to each element and can be measured.

❖ **Instrumentation:** It consists of four main components-

- a) Light source- Continuous light is emitted of broad range wavelengthseg. Hollow cathode lamp
- b) Atomization system- This system is responsible for producing free metal atoms for analysis and detection. Sample is kept into the flame for atomization.
- c) Monochromator- It allows to pass a specific wavelength through it that only required element is detected.
- d) Detector- It changes light signals to electrical signals proportional to light intensity. Example: Photomultiplier tube, Charge coupled device(CCD) detectors.

❖ **Working:** The sample in solid or liquid form is atomized with the help of flame. Due to atomization of sample free atoms are formed. These free atoms are then subjected to light emitted from hollow cathode lamp. This emitted radiation causes the transition of free atoms from ground state to energized state. The

light discharged by the light is begun from invigorated particles of a similar component being broke down. Thus, the energy of the radiation straightforwardly relates to the frequency consumed by the atomized element. After atomization of sample, light rays enter the monochromator through which light of specific wavelength passes through and reaches the detector. A calibration curve is generated by analyzing multiple samples of known concentrations under identical conditions as those used for unknown samples(Kabita Sharma 2023, n.d.)[42].

❖ **Applications:**

- a) Determination of trace elements
- b) Used in metallurgy, alloys and in inorganic analysis
- c) Pharmaceutical analysis: estimation of zinc in insulin preparation

5.1.4 UV-Vis Spectroscopy



Fig 5.4: UV-Visible Spectrophotometer

UV-Noticeable spectroscopy is a technique utilized for examination that decides the quantity of unmistakable frequencies of UV or apparent light that an example either retains or goes through rather than a references or clear example. The example piece can impact this trademark, which can give knowledge into the items and grouping of the example.

- ❖ **Principle:** UV follows the Lager Lambert's regulation, which expresses that the decline in radiation force as the thickness of a retaining arrangement increments is straightforwardly relative to both the occurrence radiation and the grouping of the arrangement.

$$\text{❖ } A = \log \left(\frac{I_0}{I} \right) E_0 C l$$

Where A_n is absorbance, I_0 is force of light occurrence on the example cell, I is the power of light leaving the example cell, C is the grouping of solute, l is the length of the way and E_0 addresses the molar elimination coefficient.

The law implies that the more prominent the quantity of particles fit for retaining light of a given frequency, the more noteworthy the degree of light retention.

❖ **Working:**

1. **Light source:** Single Xenon light is utilized as a strong wellspring of light for both the UV and noticeable reaches. Nonetheless, xenon lights are more costly and less steady than tungsten and incandescent lights. Instruments that use two lights normally utilize a tungsten or incandescent light for the noticeable reach and a deuterium light for the UV range.
2. **Wavelength selection:** The following stage in the process includes choosing explicit frequencies of light that are suitable for the example and the examinations being recognized from the wide scope of frequencies delivered by the light source.
3. **Sample analysis:** After the frequency choice cycle in the spectrophotometer, the light is coordinated through the example. It is crucial for measure a reference test, otherwise called the clear example, close by the genuine example for all investigations.
4. **Detector:** When the light has crossed over the example, an indicator is utilized to change the light into an electronic sign that can be perused. After the age of electric flow, the sign is identified and communicated to a PC or screen for yield.

5.2 Materials and reagents

Table 5.1: List of chemicals/reagents

Sr. No.	Chemicals	Company
1.	Graphene oxide	Shilpent Shilpa Enterprises, India
2.	Toluene	Avantor
3.	APTES	SRL
4.	Adipate oil	TCI Japan
5.	Kolliphorel	SIGMA-ALDRICH
6.	Xanthum Gum	CDH, Delhi
7.	Glycerol	CDH, Delhi

Table 5.2: List of instruments

S No.	Instruments	Company
1.	Sonicator	Branson
2.	Weighing Balance	Mettler Toledo
3.	Centrifuge	Remi Neya 16 R
4.	Shaker	Fine- PCR
5.	FTIR	Thermo Scientific, Germany
6.	Fluorescence spectrometer	Perkin Elmer FL6500K, Germany
7.	UV spectrophotometer	Specord 250Plus, Germany
8.	FE-SEM	Carl Zeiss Microscopy
9.	Zeta potential analyzer	Malvern DLS, Zetasizer-ZS90,UK
10.	Optical microscope	Lmi microscope
11.	Rheometer	MCR102, Anton Paar, Germany
12.	Differential examining calorimetry	DSC6000,"Perkin Elmer,USA
13.	Contact angle	C601, Kino, USA

Table 5.3: Rundown of dishes and plasticwares

S. No.	Glasswares and plasticwares
1.	Pipette
2.	Burette
3.	Beakers
4.	Measuring Cylinder
5.	Falcon
6.	Eppendorf
7.	Conical flasks
8.	Glass slide

5.3 Methodology

5.3.1 Synthesis of sGO from GO

For the silanization of graphene oxide (GO), APTES (3-aminopropyltriethoxysilane) was selected as the silane precursor. Firstly, 500mg of GO was scattered in 200 ml of toluene and saved at ultrasonication for 30 minutes to obtain a suspension. Subsequently, APTES (3100 μ l) was added dropwise to this suspension and was then kept for overnight stirring. The resulting suspension was centrifuged and washed 3 times with toluene to remove any unbound APTES and dried at in oven at 50 °C (Vuppaladadium et al., 2020)[75].

STEP-1:



STEP-2:

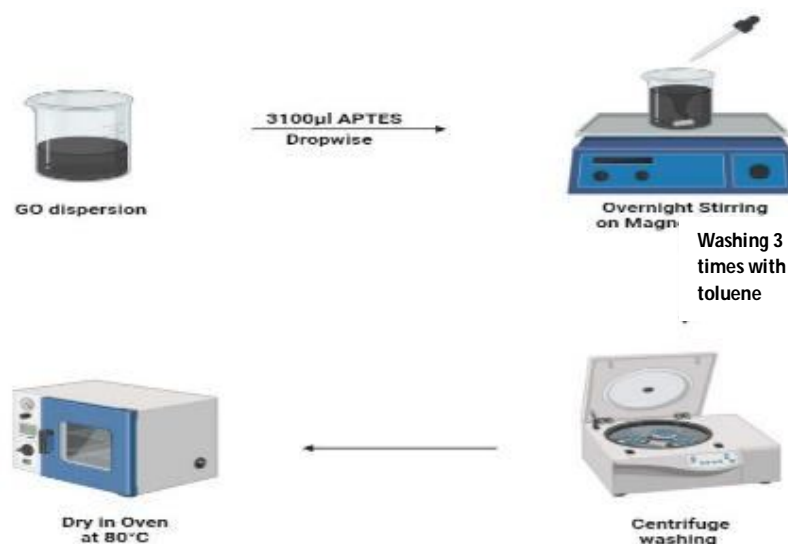


Fig 5.6: Synthesis of sGO

5.3.2 Pre-formulation study of GO and sGO

5.3.2.1 Fourier Change Infrared Spectroscopy(FTIR)

FTIR analysis employed to analyse presence or absence functional groups-GO and sGO. The functional group was studied by Thermo scientific FTIR model NICOLET iS5. Dried solid samples were prepared using KBr and were pelletized and the samples were scanned in the range from 4000cm^{-1} to 400cm^{-1} for obtaining the FTIR spectra(Jiang et al., 2019)[40].

5.3.2.2 Thermogravimetric analysis (TGA)

To evaluate the thermal stability of GO and sGO, TGA analysis was performed by heating the samples under N_2 atmosphere to 800°C at a rate of $10^\circ\text{C min}^{-1}$. (Elgendy, 2019)

5.3.2.3 Field discharge filtering electron microscopy (FESEM)

FE-EM pics of synthesized derivatives were collected on the ZEISS SUPRATM 55 SEM instrument. (Elgendy, 2019)

5.3.2.4 Raman Spectroscopy

Raman spectra of synthesized compounds were recorded using (Labram HR RAMAN spectrophotometer (HORIBA Scientific).

5.3.3 Adsorptive evacuation of weighty metal particles by AAS& complexation analysis by Fluorescence spectroscopy

5.3.3.1 By atomic absorption spectroscopy

Cluster adsorption tests were directed to concentrate on the impact of portion and impact of contact time on adsorption performance of sGO. All adsorption experiments were carried out using adsorbent sGO. Adsorption efficiency of sGO for Co (II) and Sr (II) particles were examined utilizing watery arrangements of these metal particles. The adsorbate stock arrangement (1000ppm) was ready by dissolving cobalt chloride hexahydrate ($\text{CoCl}_2 \cdot 6\text{H}_2\text{O}$) and strontium chloride hexahydrate ($\text{SrCl}_2 \cdot 6\text{H}_2\text{O}$) in Milli Q (Ahmadpour et al., 2010) (Huo et al., 2021) [2][36]. All experiments were performed in conical flasks. The procedures were as follows:

1. Effect of dose:

The effect of dose was determined by keeping the concentration of metal ion solutions constant and varying the dose. 200ppm, 50ml working solution of metal ions was prepared from stock solutions. Different doses of sGO i.e. 5mg, 10mg and 20mg were added in conical flasks containing 10ml of metal ion solutions and kept on shaking for 4hrs at 200rpm [62].

2. Contact time:

The effect of contact time of adsorbents with the metal ion solutions on adsorption capacity of sGO was determined at different time intervals i.e. 1hr, 2hr, 3hr, 4hr, 5hr and 6hr. 200ppm, 100ml working solutions each of $\text{CoCl}_2 \cdot 6\text{H}_2\text{O}$ and $\text{SrCl}_2 \cdot 6\text{H}_2\text{O}$ was prepared from stock solutions. 10ml of these metal ion solutions with 10mg dose of sGO in each conical flask were continuously shaken on thermostatic shaker for 6hours at room temperature at 200rpm. The flasks were withdrawn at predetermined time intervals from the shaker for result analysis.

All the samples were centrifuged after the experimental procedure for 5 minutes and 1ml supernatant was collected from each sample. This supernatant was then diluted with 9ml of 5% HNO_3 . Then the adsorption capacity of sGO depending on various factors was measured by Atomic Absorption Spectrophotometer ZA3000 Series, Japan.

The adsorption limit q_e (mg g^{-1}) and the evacuation adequacy still up in the air by the accompanying condition:

$$\text{Evacuation \%} = R = (C_0 - C_e) * 100 / C_0;$$

$$q_e = (C_0 - C_e) * V / m$$

where V (Liters) is the volume of the metal particle arrangement, m (g) is the heaviness of the permeable, and C₀ and C_e is the underlying and the last focus (mg L⁻¹) of metal particles in the aqueous solution (Einollahi Peer et al., 2018)[28].

5.3.3.2 By fluorescence spectroscopy

Adsorption capacity of silanized graphene oxide was assessed by fluorescence spectroscopy using Perkin Elmer FL6500K spectrophotometer. Firstly, 20mg of sGO was dispersed in 10ml of milli Q and kept on sonication for 2hours to get a fine dispersion. This dispersion was then filtered out using syringe filter and further used for fluorescence study. 3ml of sGO dispersion was taken in cuvette and fluorescence spectra was recorded. After this subsequently, 10-10 μ l of Co⁺² or Sr⁺² ion solution was added in cuvette till 100 μ l concentration and spectra was recorded at each addition step.

5.3.4 Synthesis of GO and sGO based Pickering emulgels

5.3.4.1 Preparation of GO/sGO suspension (aqueous phase)

The GO/sGO aqueous suspensions were formulated by dispersing GO/sGO in distilled water. Then, the prepared suspension was kept on probe sonication for 5 minutes.

5.3.4.2 Prep. of oil phase

The oil phase was prepared by dissolving kolliphorel and adipate oil. Firstly, required quantities of adipate oil and kolliphorel were heated in separate beakers at 70°C for 10-15 minutes. Then adipate oil was added to the beaker containing kolliphorel and stirred well. Then hot water was added (maintained at the temperature same as oil) to this oil phase under homogenization at low speed to obtain a hazy solution.

5.3.4.3 Preparation of thickening phase

The thickening phase was prepared by dissolving xanthum gum and glycerol. Both these agents were mixed well and water heated upto 70°C was added to this phase with continuous stirring to obtain a slurry.

5.3.4.4 Preparation of GO pickering emulgel

The oily phase was gradually added to the thickening phase while continuously stirring with a glass rod until it cooled down to room temperature. Then this mixture was homogenized for proper mixing to form a clear emulgel formulation. After this, the

above formulation was added to the GO/sGO aqueous suspension and kept on homogenization for 2 hours(DAOOD et al., 2019)(Warning, 2018)[18][76].

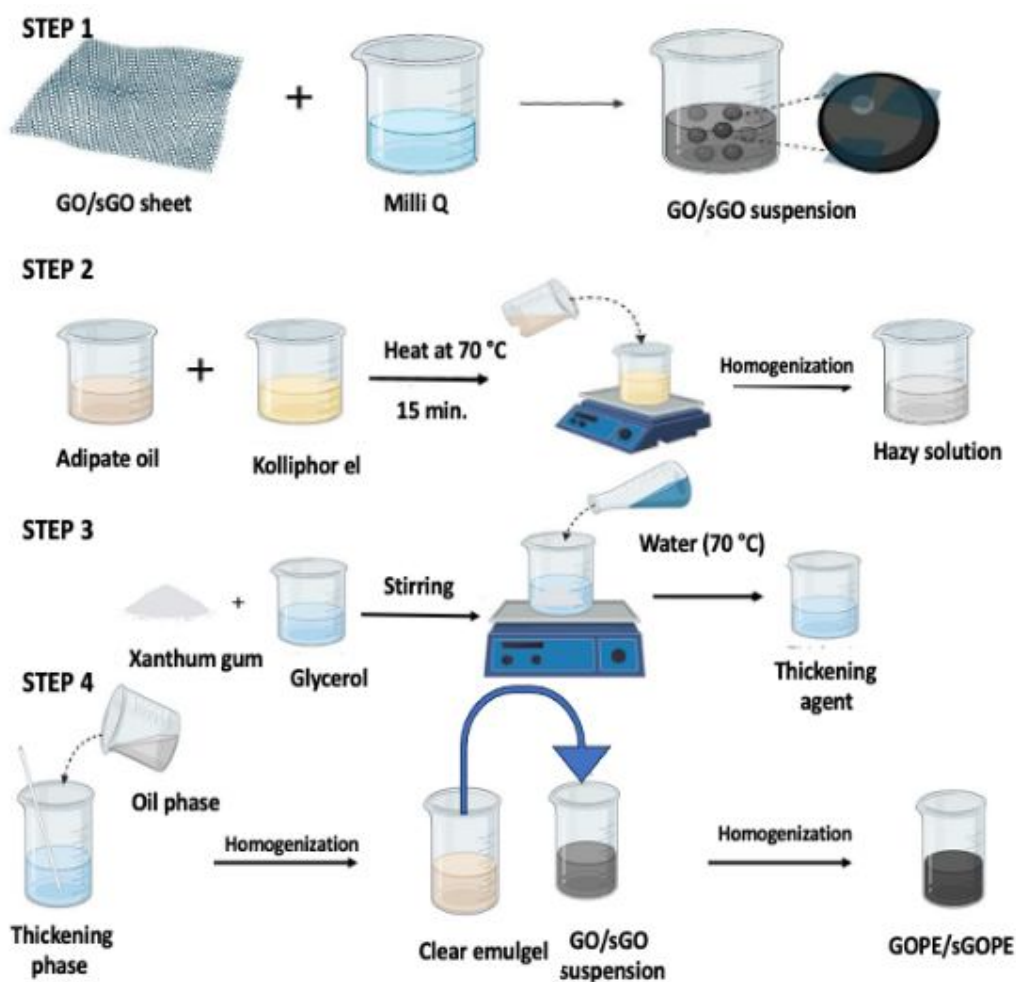


Fig 5.7: Steps for synthesis of GOPE/Sgope

5.3.5 Physiochemical characterization of GOPE and sGOPE

5.3.5.1 Physical appearance

The prepared PE formulations were visually examined for color, odor, homogeneity, grittiness, consistency and phase separation.

5.3.5.2 pH Determine

The pH of prepared PE formulation determined by utilizing advanced pH meter. It was assessed by positioning the digital pH meter in the prepared formulation and allowed it to equilibrate for 1 minute and subsequently recorded the readings in triplicates[24].

5.3.5.3 Molecule size and polydispersity list (PDI)

Molecule size examination is an important parameter to characterize the emulgel. DLS, a widely utilized method, measures the size distribution of particles by assessing fluctuations in light scattering resulting from Brownian motion. Laser diffraction is another common technique that determines particle size distribution based on the diffraction of laser light by particles in the emulsion. Additionally, microscopy proves valuable in visualizing both the size and shape of particles within the emulsion (Bao et al., 2021)[8].

5.3.5.4 Zeta Potential

Zeta potential examination is performed to evaluate the surface charge of particles within formulation. It provides information regarding the stability of the emulgel by indicating the attractive and awful powers among the particles. A high negative or positive zeta potential signifies effective particle dispersion, indicating stability in the Pickering emulgel. Whereas, a low zeta potential indicates a tendency for particle aggregation, signifying instability in the Pickering emulgel(Donthi et al., 2023)[24].

The formulated emulgels were introduced into the sample cell that was equilibrated at 25 °C for 2 min, and then zeta potential was estimated utilizing a zeta expected analyser, Malvern DLS, Zetasizer-ZS90, UK.

5.3.5.5 Optical microscopy

Optical microscopy is a valuable method for examining the structural aspects of Pickering emulgel. This technique facilitates the observation of droplet characteristics such as size, shape, and distribution, offering insights into the impact of particles on the stability of the Pickering emulgels.

The prepared Pickering emulgels were examined under a light microscope equipped with a digital camera LMI microscope, LEEDZ microimaging Ltd. The images obtained were analysed. For this observation, approximately 0.01 ml of emulsion samples, both before and after high-pressure homogenization and stabilized for 1 day, were applied onto a glass slide and covered with a coverslip. Following a 30-minute equilibration period, the samples were analysed at room temperature under 20x magnification(Li & Xiang, 2019)[46].

5.3.5.6 Rheological studies

Rheological analysis is a method to study the flow characteristics of the formulations. Rheological properties of materials describe how the concentrations of excipients, such as oils, surfactants, and gelling agents, impact the viscoelastic flow behaviour of a formulation. Variations in viscosity and flow characteristics within the formulation can potentially affect its stability, drug release, and other in-vivo parameters. Emulgels with higher viscosity tend to exhibit greater stability compared to those with lower viscosity. Techniques such as oscillatory rheology and steady-state shear rheology can be employed for rheological analysis(Donthi et al., 2023)[24].

The rheology of the formulated emulgel was determined using MCR102, Anton Paar Rheometer, Germany and data was analysed using RHEOCOMPASS software. The instrument had shaft disc of 25 mm and base disc of 55 mm. The small amount of emulgel was poured onto the base disc in concentric circular form. The shaft disc was placed above base disc with a disc gap of 1 mm and temperature was kept at 25°C. Shaft movement was performed till it reached 1N force. This was followed by running the viscosity curve program, amplitude and frequency sweep scan. The readings for rheological parameters were recorded and analysed.

5.3.5.7 Differential Checking Calorimetry (DSC)

Differential Checking Calorimetry is a warm examination device that identifies changes in the actual properties of an example with connection to temperature after some time Scanning Calorimetry (DSC). As temperature shift occurs, DSC quantifies the heat exchanged—whether radiated or absorbed—by the sample, based on the temperature distinctions between the example and a reference material(Ebert et al., 2017)[26]. The DSC was carried out using DSC 6000, Perkin Elmer, USA apparatus.10mg of formulated emulgel was placed in aluminium pan and sealed hermetically. Then the sealed pan was positioned within the thermocouples of the calorimeter. The emulgel underwent a heating process from 20°C to 60°C atrate of 5°C/minute. After reaching 60°C, the emulgel was equilibrated at this temperature. Following this, the sample was cooled down to -60°C using the same incremental process and equilibrated at -60°C. Then, the sample was reheated to 60°C at a rate of 5°C per minute.

5.3.5.8 FT-IR

The infrared spectra of GO, sGO, xanthum gum, kolliphorel, adipate oil, glycerol, GOPE and sGOPE were recorded in the range of 400 to 4000 cm^{-1} to identify various functional moieties. All the powdered samples were mixed in the ratio of 1:100 with dried powdered potassium bromide (KBr). First, the mixture was finely ground into a powder using a mortar and pestle and triturated. It was then compacted into KBr circles involving a water driven press at 10,000 psi for 30 seconds each. Each KBr circle was filtered using Thermo Scientific IR software OMNIC, from wavenumber range of 4000–400 cm^{-1} at a scanning rate of 4 mm/s and a path length of 2cm. The liquid samples however were analysed using the ATR accessory of the FT-IR. The characteristic peaks were recorded and comparative analysis was done to detect any possible changes in the peaks of the spectra (DAOOD et al., 2019)[18].

5.3.5.9 Contact Angle Determination

Contact angle is a property used to determine the surface characteristics which includes surface energy or adhesion energy. The contact points of the examples were estimated using static and dynamic contact angle meter (C601, Kino Industry, USA). The GO and sGO emulgels were applied onto the glass slide. Further, the surface was coated with adipate oil and positioned on the sample table. After 5 s equilibration time period, the image of droplet was captured by a high-speed camera. The droplet's profile was then analyzed numerically and fitted automatically to the Laplace Young equation to determine the contact angle. (Bao et al., 2021)[8].

5.3.5.10 FE-SEM analysis

SEM images of synthesized derivatives were collected on the ZEISS SUPRATM 55 SEM instrument.

5.3.5.11 Stability Studies

The stability assessment of GO and sGO were performed according to the guidelines set forth in the International Conference on Harmonization (ICH), Q1A (R2) guideline, 2003. In this particular study, the prepared formulations were examined under following storage conditions: ($8^{\circ}\text{C} \pm 2^{\circ}\text{C}$, $25^{\circ}\text{C} \pm 2^{\circ}\text{C}$, $40^{\circ}\text{C} \pm 2^{\circ}\text{C}$)/60 %RH \pm 5%RH, for a time span of 90 days. The goal of this study was to research effect of these varied storage

conditions on key properties of the emulsion, including colour, appearance, pH, and phase separation, throughout specific time intervals.

5.3.6 Evaluation of decontamination efficacy of PE

5.3.6.1 Preparation of animals

SD rats are a common laboratory animal model used in scientific research. For this particular study, the dorsal side of rats will be shaved with a diameter of 2 cm. This will be probably done to maintain uniformity in the region under investigation and to lessen any potential confounding influences that hair might have brought. The rats are then placed in an animal facility under natural lighting conditions after being shaved. To assure their welfare and reduce any potential stress, the rats should be placed in a controlled environment with regulated temperature, humidity, and lighting settings.

5.3.6.2 Decontamination procedure

The dorsal surface of the skin of SD rats is shaved and marked with 3 cm diameter circle. The ketamine: xylazine cocktail is used to anesthetize rats for decontamination studies. The area is contaminated with 100 µl of heavy metal ion solution using disposable plastic syringe on the marked surface area of the skin and is air dried and left for 5 minutes. The animals are grouped into four groups with each group consisting of six animals. The decontamination of heavy metal ions is performed using cotton swabs (2cm radius) after soaking with 2 ml of decontaminant. For group 1 no decon is performed, for group 2 MilliQ water with soap solution is used for decon, for group 3 GOPE and for group 4 sGOPE are used for decontamination. The decontamination is carried out starting from the periphery of the circle to the centre. Whole body counter is used for recording the radiation counts in case of heavy metals exposure. The decontamination efficiency was expressed in terms of a percentage of the removed contaminant by using the following formula;

$$\text{Decontamination efficiency (\%)} = \frac{C_o - C_e}{C_o} \times 100$$

Where C_o is the contamination level before application, and C_e is the contamination level after application (Li et al., 2017)(Rana et al., 2014a)[58].

CHAPTER-6
RESULTS AND DISCUSSION

CHAPTER-6

RESULTS & DISCUSSION

6.1 Characterization of GO & sGO

6.1.1 Fourier Change Infrared Spectroscopy (FTIR)

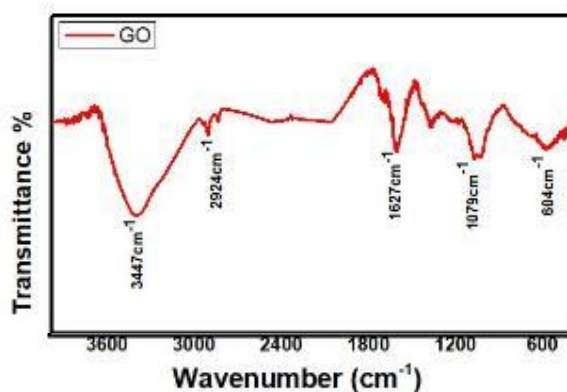


Fig 6.1: FTIR spectrum of GO

FTIR spectrum of graphene oxide (GO) was utilized to analyze the existence of several functional groups integrated into the GO surface subsequent to the oxidation of graphite (Berthomieu & Hienerwadel, 2009)[10]. The different IR bands of GO were shown by the FTIR spectra at 1079cm^{-1} , 1627cm^{-1} , 2924cm^{-1} , and 3447cm^{-1} . The extending recurrence of C-O was gotten at 1079cm^{-1} . Likewise, the extending recurrence of C=O (amide) was obtained at 1627cm^{-1} , the bending frequency of C-H was acquired at 2924cm^{-1} , and the skeleton vibration of the O-H was identified at 3447cm^{-1} .

Table 6.1: FTIR peaks of GO

Functional groups	Reported peaks	Peaks
O-H	3350-3650	3447
C-H	2840-2950	2924
C=O	1500-1700	1627
C-O	1036-1382	1079

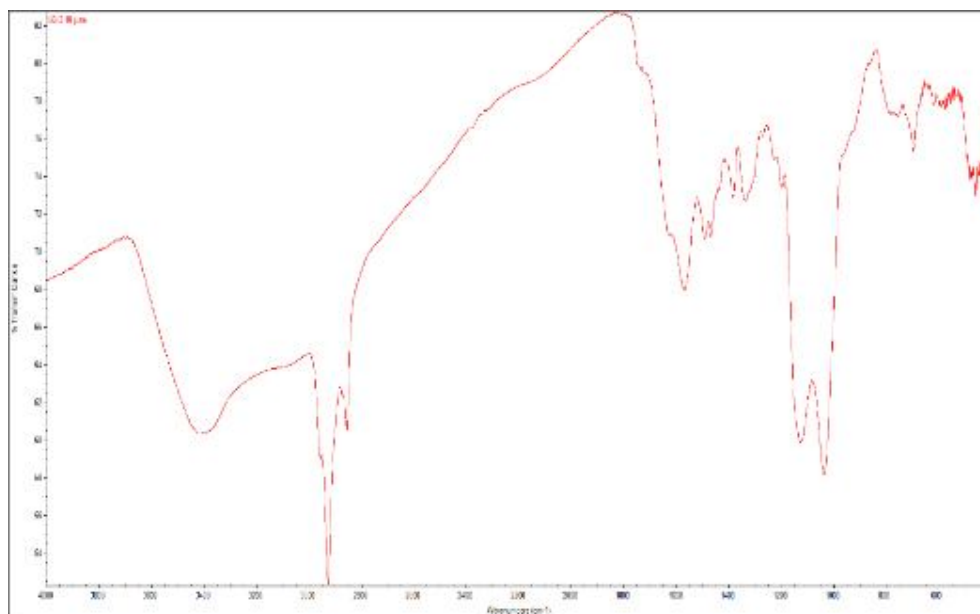


Fig 6.2: FTIR spectra of sGO

In the sGO FTIR scan, a broad absorption band with a peak at 2983 cm^{-1} indicates C-H bond vibrations originating from CH_2 and CH_3 groups. A top at 2140 cm^{-1} relates to the extending vibration of the C-H bond. A little top around 1590 cm^{-1} demonstrates the lopsided extending of C=C securities in the fragrant ring. The top at 1290 cm^{-1} is because of the extending vibration of the C-N bunch, while the top around 700 cm^{-1} relates to Si-phenyl compounds(Prodan et al., 2021)[56].

Table 6.2: FTIR peaks of sGO

Functional groups	Reported peaks	Observed Peaks
O-H	3350-3650	3395
C-H (bond vibration)	2840-2950	2983
C-N	2138-2330	2140
Silane group	1930-2047	1918
C=C	1540-1600	1590

6.1.2 Thermogravimetric analysis (TGA)

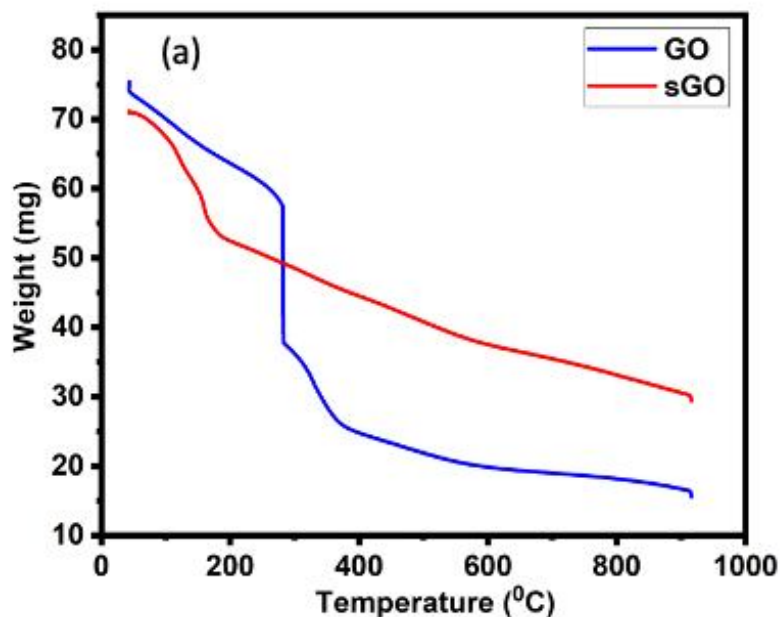


Fig 6.3: TGA of GO and sGO

Thermogravimetric examination was utilized to explore the thermal stability of graphene oxide (GO) and surface-changed graphene oxide (sGO). GO showed huge mass loss beginning underneath 200°C, basically because of the arrival of adsorbed water and the decomposition of oxygen-containing groups like hydroxyl and carboxyl. As the temperature increased, the mass loss intensified: around 20% below 100°C due to water loss, approximately 30% at 200°C from the degradation of oxygenated groups, and up to 40% at 500°C attributed to the combustion of the carbon skeleton. Complete combustion of GO occurred around 800°C.

In contrast, TGA of sGO revealed a different thermal behavior. The presence of silane groups on its surface caused weight loss between 180-580°C, with about 15% mass loss below 200°C primarily due to water loss, and an additional 25% up to 800°C due to significant burning and pyrolysis of the carbon skeleton. The gradual changes observed in the sGO thermograms indicated higher stability compared to GO under thermal conditions (Fraga et al., 2020) (Toorchi et al., 2022) [32][69].

6.1.3 Field outflow examining electron microscopy (FESEM)

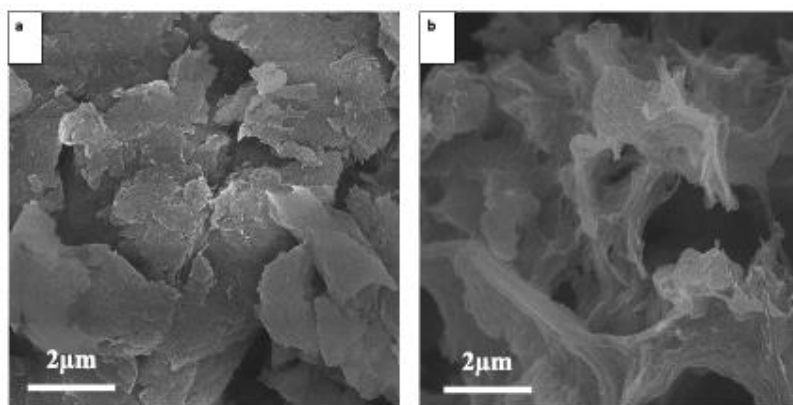


Fig 6.4: FE-SEM images of (a) GO and (b) sGO

The SEM analysis of GO revealed rough, layered sheets with creased and crumpled edges, indicating the presence of functional groups. Translucent regions showed oxygen moieties distributed on the graphene lattice. The aggregation at various sites revealed its multilayered structure.

To evaluate any significant changes due to silanization, the morphological properties of sGO were investigated. The flaky morphology showed wrinkles and a multi-layered structure, but there were no significant changes in length and thickness post-silanization.

The increased number of wrinkles in sGO could be due to the presence of APTES between the layers i.e. due to silanization(Vuppaladadiam et al., 2020)[75].

6.1.4 Raman Spectroscopy

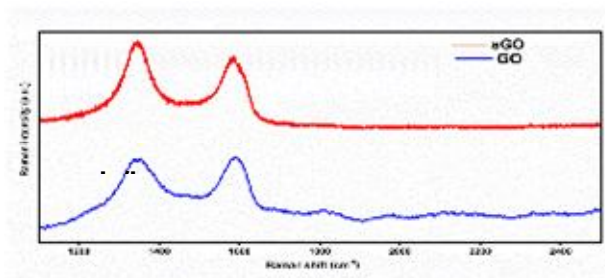


Fig 6.5: Raman spectra of (a) GO and (b) sGO

The Raman spectra of graphene nanocomposites show two distinguished vibration peaks known as the D and G bands. The G band corresponds to in-plane vibrational mode because of sp^2 -hybridized carbon atoms. In contrast, the D band indicates structural and surface defects due to out-of-plane vibrational modes. The power proportion of both the groups (I_D/I_G) is utilized to decide the degree of confusion in the graphene precious stone cross sectio. A higher I_D/I_G ratio signifies greater structural disorder and deformation of the graphene layers(Vuppaladadium et al., 2020)(Rahman et al.,2022)[75].

In Raman spectrum of GO, peaks of D&G bands occurred at 1348cm^{-1} & 1602cm^{-1} , respectively, with a band intensity ratio (I_D/I_G) of 0.84. For sGO, the D and G band peaks were observed at 1290cm^{-1} and 1410cm^{-1} , respectively, with an I_D/I_G proportion of 0.91. I_D/I_G proportion expanded from 0.84 for GO to 0.91 for sGO that indicates greater structural disorder and deformation of the graphene layers after silanization with APTES.

6.2 Adsorptive evacuation of weighty metal particles by AAS & complexation analysis by Fluorescence spectroscopy

6.2.1 By Nuclear Assimilation Spectroscopy

6.2.1.1 Effect of dose

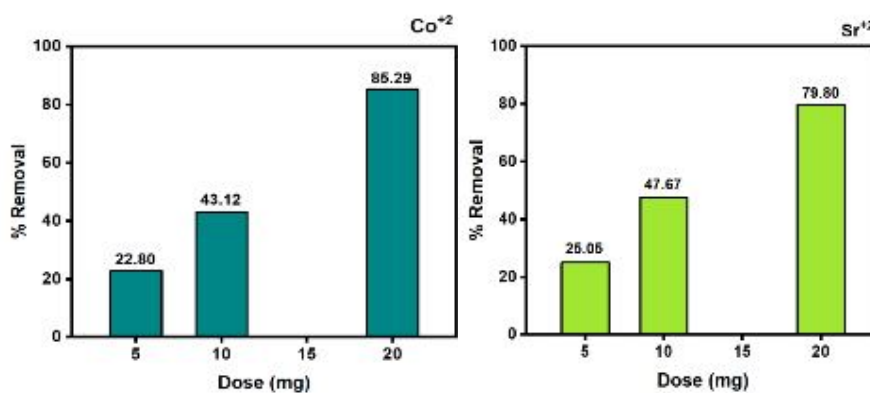


Fig 6.6: Effect of dose on adsorptive efficacy of sGO for (a) Cobalt (b) Strontium

Effect of dose on adsorption capacity of sGO was investigated by varying the dose of adsorbent i.e. 5mg, 10mg and 20mg in 3 different conical flasks containing 10ml of heavy metal ion solution. When the dose of sGO was increased from 5mg to 20mg, % evacuation of Co(II) and Sr(II) increased to a greater extent as seen from the above graphs.

The removal percentage of Co (II) ions increased from 22.80 at 5mg dose to 85.29 at 20mg dose indicating good adsorption capacity at higher doses. Similarly, the removal percentage of Sr (II) ions increased from 25.05 at 5mg dose to 79.80 at 20mg dose of sGO. The significant improvements in removing metal ions can be associated to the bigger number of restricting locales on a superficial level of silanized graphene oxide due to functionalization of GO.

Also, it is evident from above graphs that sGO showed better adsorptive removal of cobalt ions i.e. 85.29% than strontium ions which is 79.80% from the aqueous solution of heavy metal ions.

6.2.1.2 Impact of contact time

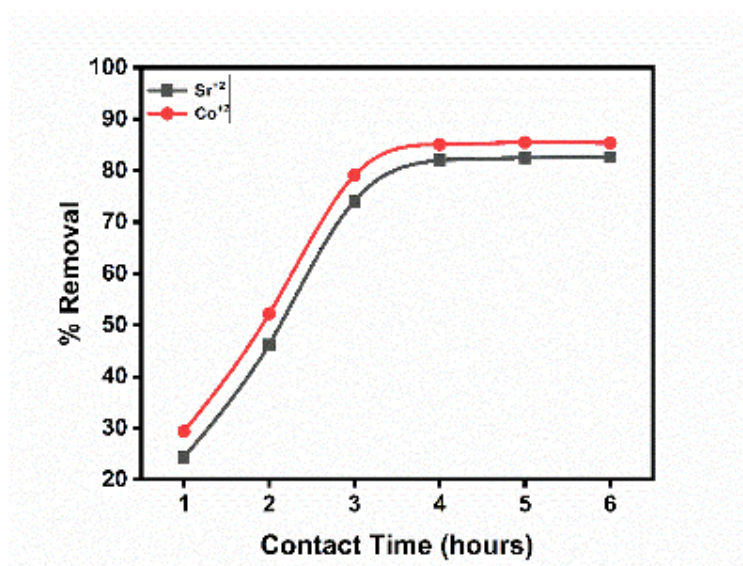


Fig 6.7: Impact of contact time on adsorption efficacy of sGO for Co⁺² and Sr⁺²

The graph shows the percentage removal of Sr²⁺ and Co²⁺ ions by sGO over a contact time of six hours. Both Sr²⁺ and Co²⁺ ions show significant removal within the first hour. Co²⁺ removal starts slightly higher than Sr²⁺. There is a rapid increase in the removal percentage for both ions from the first to the third hour. Co²⁺ shows a faster and slightly higher removal rate compared to Sr²⁺. After three hours, the removal rate for both ions starts to plateau.

Co^{2+} reaches about 90% removal by the fourth hour and remains stable. Sr^{2+} reaches approximately 85% removal by the fourth hour and also stabilizes. At the end of six hours, Co^{2+} achieves around 90% removal efficiency and Sr^{2+} achieves around 85% removal efficiency. sGO is highly effective in adsorbing both Sr^{2+} and Co^{2+} ions from the solution. Co^{2+} ions are removed slightly more efficiently and faster than Sr^{2+} ions. The adsorption process reaches equilibrium for both ions around three to four hours. This indicates that sGO can be a promising material for the removal of these heavy metal ions, with Co^{2+} being slightly more efficiently removed than Sr^{2+} .

6.2.2 Complexation analysis by Fluorescence spectroscopy

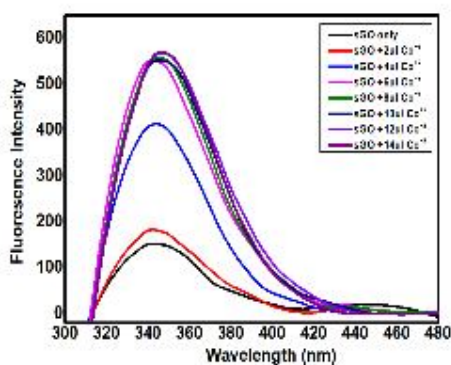


Fig 6.8: Fluorescence spectra of sGO with Co^{+2} ions

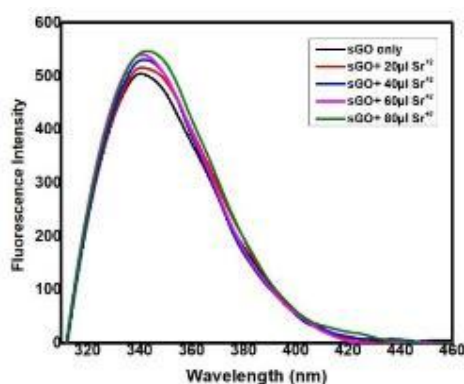


Fig 6.9: Fluorescence spectra of sGO with Sr^{+2}

The fluorescence spectroscopy was performed to analyze the complexation behaviour of sGO with heavy metal ions. Different volumes of Co^{2+} (ranging from 2 μL to 14 μL) and Sr^{2+} (ranging from 20 μL to 80 μL) ions solutions have been added to the sGO, resulting in various changes in fluorescence intensity.

In both graphs (**fig 6.8 & fig 6.9**), the addition of metal ions (Co^{2+} and Sr^{2+}) to the sGO solution results in an increase in fluorescence intensity. As the volume of Co^{2+} increases from 2 μL to 14 μL and that of Sr^{2+} increases from 20 to 80 μL , there is significant increase in fluorescence intensity, reaching a maximum with 14 μL of Co^{2+} and with 80 μL of Sr^{2+} . This increase in fluorescence intensity indicates that the metal ions are binding to the free surface of sGO, which likely alters the electronic environment of the sGO, resulting in enhanced fluorescence.

The fluorescence intensity increases more significantly with the addition of Co^{2+} compared to Sr^{2+} . This suggests that the interaction between sGO and Co^{2+} is stronger or more efficient than that with Sr^{2+} . This can be due to factors such as the size, charge, or specific affinity of Co^{2+} ions to the functional groups on sGO.

The capacity of sGO to bind with heavy metal ions makes it useful for cleaning up the environment, purifying water, and detecting heavy metals. The way sGO binds to different metals means it can be used to specifically remove or detect certain metal ions.

6.3 Physicochemical characterization of GOPE and sGOPE

6.3.1 Physical Characteristics:

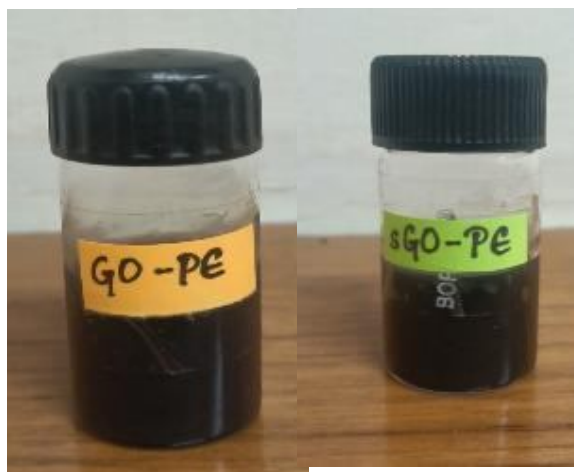


Fig 6.10: Appearance of GOPE and sGOPE

The physical and substance properties of the emulgel are shown in table 6.1.

Table 6.3: The physical and chemical properties of Emulgel

	Colour	Odour	Texture	pH
GOPE	Greyish black	odorless	Smooth homogenous Pickering emulgel	7.9±0.003
sGOPE	Greyish black	odorless	Smooth homogenous Pickering emulgel	6.08±0.02

6.3.2 pH Determination:

The pH of sGOPE was 6.08 ± 0.02 and that of GOPE was 7.9 ± 0.003 . The obtained pH values were within the acceptable range for topical applications, indicating that these are unlikely to cause any skin irritation. As per the previous studies it was found that pH in the range of 5 to 7.5 was acceptable for topical application (Rana et al., 2014b) [59].

6.3.3 Particle size analysis of emulgels:

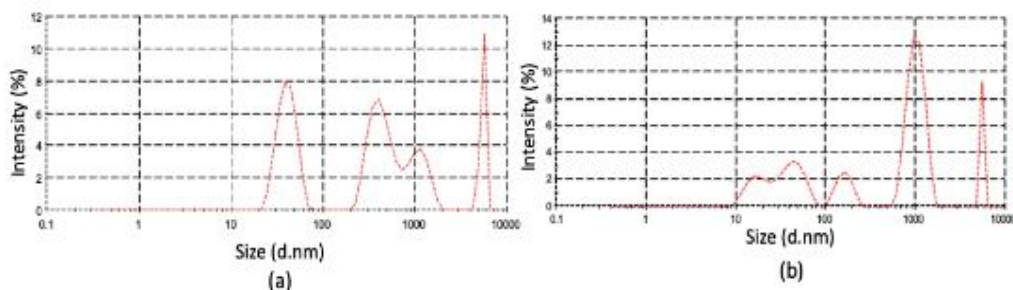


Fig 6.11: Size analysis of (a)GOPE and (b) sGOPE

The DLS of GOPE revealed the size to be 518.9 nm as shown in **fig 6.11(a)**. The DLS of sGOPE revealed the size to be 962 nm as shown in **fig 6.11(b)**.

6.3.4 Zeta Potential analysis:

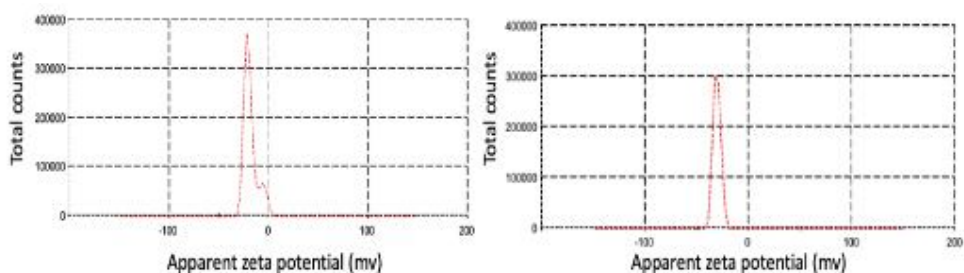


Fig 6.12: Zeta Potential of (a) GOPE and (b) sGOPE

Particles with a zeta potential under +30 mV or more negative than - 30 mV are by and large thought to be as steady. Zeta potential of GO-based pickering emulgel was found to be $-21.5 \pm 2.5\text{mV}$ as shown in **fig 6.12(a)**, which indicates that droplets of GOPE have negative charge which is closer to range where stable PE is formed.

The zeta potential -18.5 was observed for sGOPE as shown in **fig 6.12(b)**. The results are indicative of functionalization of GO with APTES, that lead to the increase in positive charge in sGOPE as well the bulkier group in sGOPE increased the average size as well.

6.3.5 Optical microscopy:

The microscopic images of emulgels were recorded at 20 X magnification (**Fig 6.13**). The images revealed the even distribution of GO and sGO particles in the emulgel. Also, the microscopic images showed homogenous emulgels are synthesized.

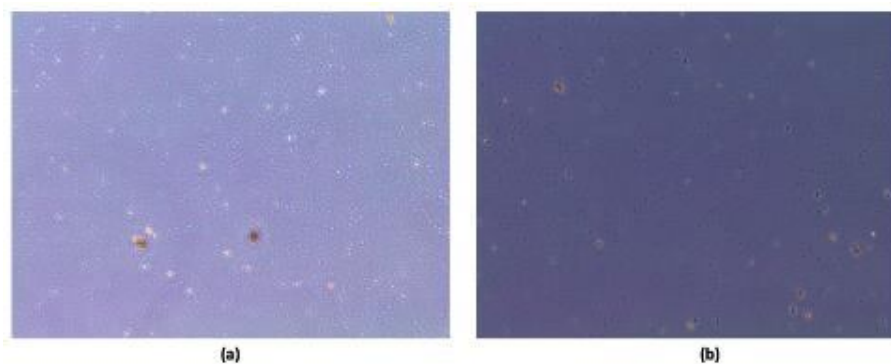


Fig6.13: Optical microscopic images of (a) GOPE and (b) sGOPE at 20X magnification

6.3.6 Rheology of pickering emulgel:

The flow curves were obtained in the stress rate ranging from 0.01-100 s^{-1} in the rheological study (Moraes et al., 2020)[50].

Figure 6.14 and **fig 6.15** flow curves illustrated that, magnitude of viscosity decreases with the increasing values of shear rate and the formulated emulgel does not follow the Newton's law of viscosity indicating the non-newtonian and shear thinning flow behavior of the emulgel (Espert et al., 2022; Szymańska et al., 2023)[29][64].

Frequency sweep plot (Fig 6.16) depicted the predominance of elastic behaviour (G') over viscous behavior (G'') at varying values of angular frequency indicating the presence of stable gel-like formulation in the emulgel (Espert et al., 2022)[29].

Amplitude sweep plot (Fig 6.17) indicated that the formulated emulgel exhibited viscoelastic solid properties ($G' > G''$) suggesting physical stability (Vukašinović et al., 2023)[74].

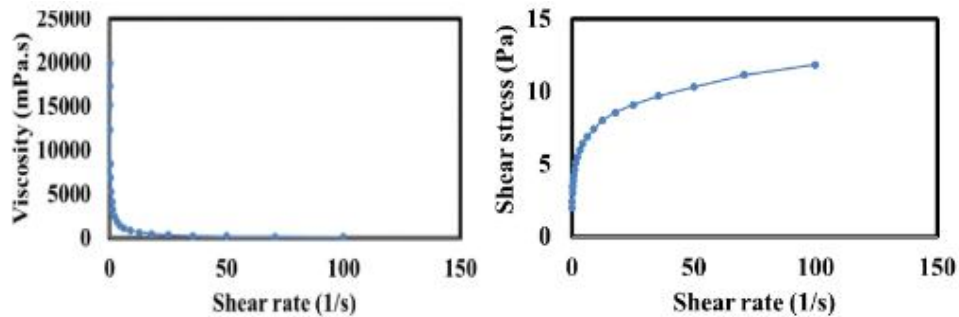


Fig 6.14: Flow curves of GOPE

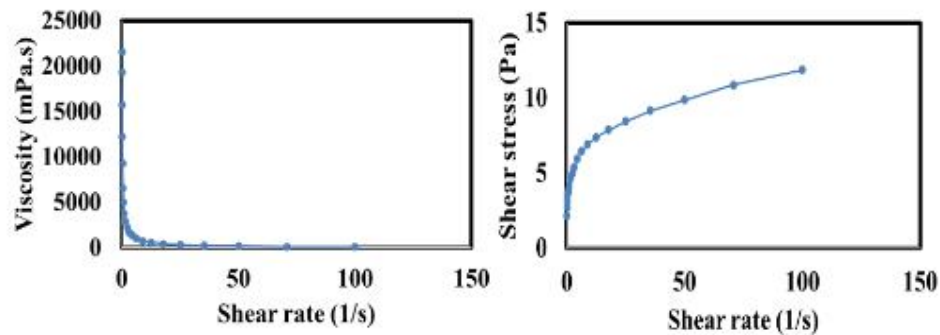


Fig 6.15: Flow curves of sGOPE

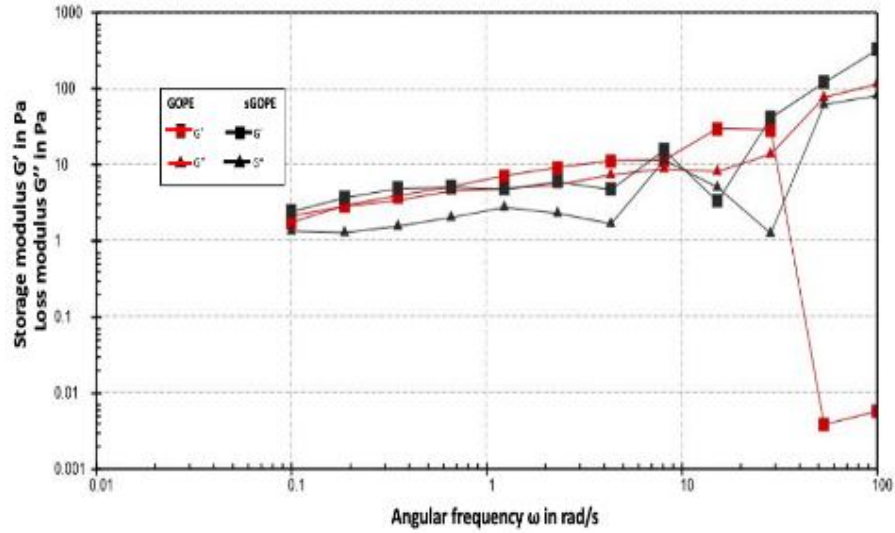


Fig 6.16: Frequency sweep plots of GOPE and sGOPE

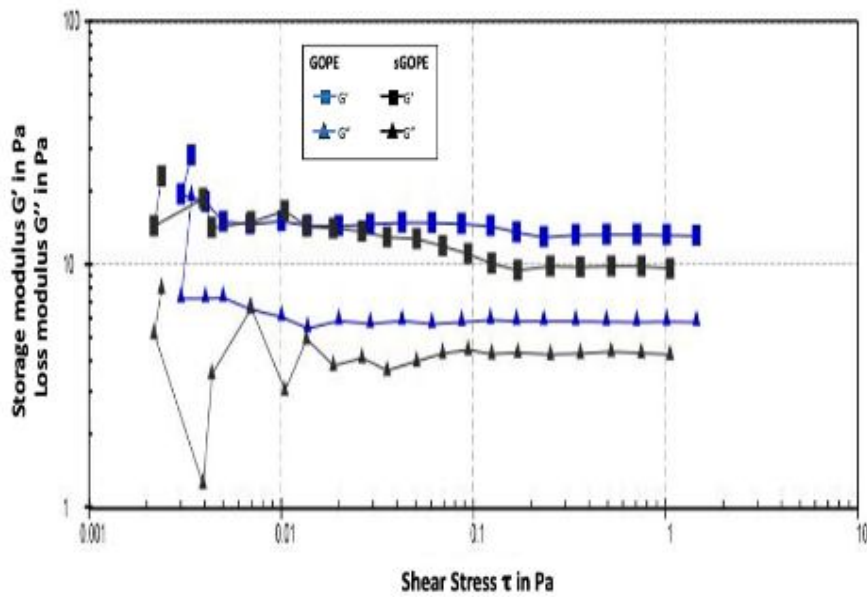


Fig 6.17: Amplitudesweep plots of GOPE and sGOPE

6.3.7 DSC analysis of pickering emulgel:

Thermal analysis of prepared pickering emulgel was determined using DSC 60 plus, Perkin Elmer, Shimadzu corporation, Japan. The results from the DSC analysis of the prepared formulation depicted an endothermic peak at 119°C as illustrated in **fig 6.18**. This analysis indicated that if temperature is increased above 119°C then formulation changes to molten state.

Thermal analysis using DSC examines how heat flows either into or out of an example as an element of temperature or time. The **Fig 6.18(a)**, showed a slight endothermic peak representing melting at approximately 90°C and a significant exothermic peak at about 230°C indicates the breakdown of oxygenated functional groups during generation of CO and CO₂ in GOPE (Alam et al., 2017)[4]. For sGOPE, an endothermic reaction through “melting” was found to be shifted slightly towards the right in comparison to GOPE as depicted by the endothermic peak shown in **Fig 6.18(b)** at approx 120°C. An exothermic peak showing crystallization similar to graphene oxide was observed at about 230°C. The results of DSC were also indicative of better stability of sGOPE as compared to GOPE.

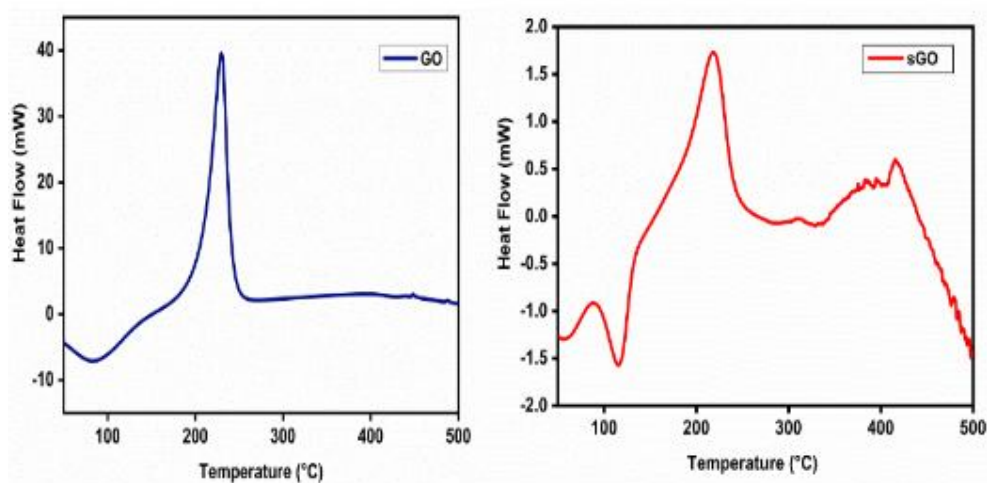


Fig 6.18: DSC curves of (a) GOPE and (b) sGOPE

6.3.8 FT-IR analysis of pickering emulgel

IR absorption spectrum of the components of PE was observed in the scope of 4000-400 cm⁻¹ utilizing KBr pellet strategy by FTIR spectrometer. The major peaks were reported to compare the results obtained as shown in **fig 6.19**. The range shows an expansive pinnacle showing up at 3402cm⁻¹ in the high recurrence region portraying the extending of O-H bond, which demonstrates the presence of hydroxyl bunch in PE detailing.

In the sGO FTIR scan, a broad absorption band with a peak at 2983 cm⁻¹ indicates C-H bond vibrations originating from CH₂ and CH₃ groups. A top at 2140 cm⁻¹ relates to the extending vibration of the C-H bond. A little top around 1590 cm⁻¹ demonstrates the

unbalanced extending of C=C securities in the sweet-smelling ring. The top at 1290 cm^{-1} is because of the extending vibration of the C-N bunch, while the top around 700 cm^{-1} corresponds to Si-phenyl compounds(Prodan et al., 2021)[56].

FTIR spectra of GO-PE depicted stretching vibration of -OH around 3324 cm^{-1} , corresponding methyl and methylene groups at 2944 cm^{-1} , -C=O (ester group)at 1735 cm^{-1} & 1637 cm^{-1} and C-O ester group at 1095 cm^{-1} indicating the presence of excipients in the emulgel. The FTIR spectra of sGOPE showed an -OH stretch around 3326 cm^{-1} , corresponding methyl and methylene groups at 2933 cm^{-1} , -C=O (ester group) at 1739 cm^{-1} & 1637 cm^{-1} and C-O (ester group) peaks between 1099 cm^{-1} & 1020 cm^{-1} . The peaks of excipients in the spectra of emulgel confirms its presence in the pickering emulgel. FTIR peaks of different components and the emulgels are shown in **table 6.2**(Almilly et al., 2023)(Fosu et al., 2016)[6][31].

Table 6.4: FTIR peaks corresponding to different functional groups of various components of pickering emulgel

<u>Functional Groups</u>	GO	sGO	GO-PE	sGO-PE	Diethyl adipate	Kolliphorel	Xanthum gum
O-H	3766	3295	3324	3326	-	3455	3288
Methyl and methylene	2950	-	2944	2933	2940	-	2933 & 2879
C=O (ester bond)		-	1735 & 1637	1739	1729	1733	1654
-COO		-	-	1467	-	-	1421 & 553
C-O (ester group)	1170	-	1095		1174	1099	
C-C			-			944	
C-N	-	1290	-	-	-	-	-
C=C		1590					

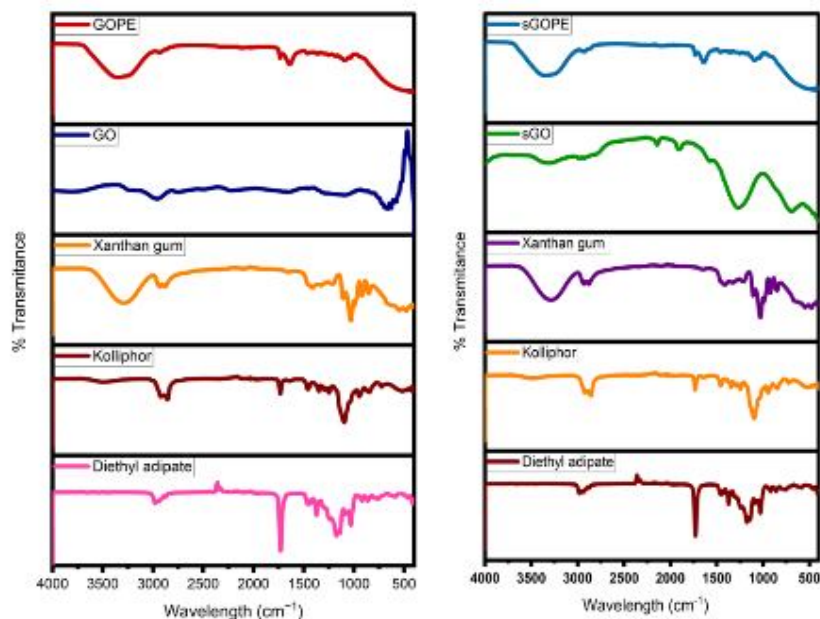


Fig 6.19:FT-IR Spectra of GOPE, sGOPE, and all the components of Emulgel

6.3.9Contact angle measurement:

Contact angle property helps to decide the emulsion type whether it is oil-in-water or water/ oil based on the value of theta (θ). Value of $\theta < 90^\circ$ indicates that particles are mostly hydrophilic and stabilize oil-in-water emulsions because greater extent of particles are in aqueous phase. Whereas, when $\theta > 90^\circ$, it indicates that particles are mostly hydrophobic and stabilize water-in-oil emulsions(Bao et al., 2021)[8].

The contact angle of the samples was measured using Kruss contact angle meter and the findings are depicted in **Fig 6.20(a)** and **Fig 6.20(b)**.



Fig 6.20: Contact angles of (a) GOPE and (b) sGOPE

The obtained contact angle (θ) for GO-based Pickering emulgel was 52.1° , while for sGO-based Pickering emulgel, it was 48.2° . These values suggest that the formed

Pickering emulgels are of oil-in-water type, as value of θ for both the emulgels is less than 90° .

6.3.10 FE-SEM

FE-SEM analysis of GOPE showed that particles of the formulation were discrete and longitudinal in shape with slight aggregation as shown in **fig6.21(a)**. FE-SEM analysis of sGOPE illustrated that particles have short curvy stretches at the surface as shown in **fig6.21(b)**.

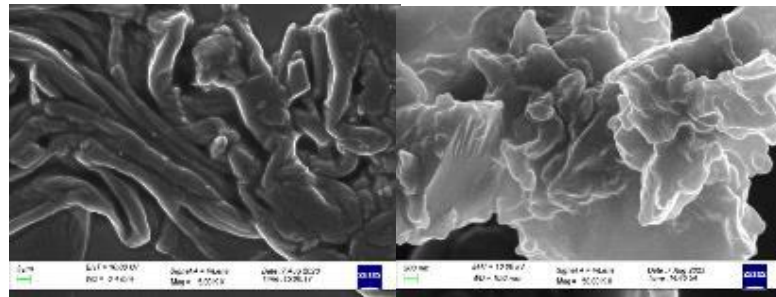


Fig 6.21: The SEM micrographs of GOPE and sGOPE at 5X magnification and 50X magnification.

6.3.11 Stability

The stability of the prepared emulgels was assessed for three months (90 days) at three different temperature conditions i.e. 8°C , 25°C and 40°C . The stability studies were indicative of stable nature of emulgel with no changes observed in appearance, minor pH variations and no phase separation. The different parameters of stability are shown in **Table 6.5**.

Table 6.5: Stability study analysis GOPE and sGOPE

Samples		Time (Days)	Color	Appearance	pH	Phase separation
GOPE	8°C ± 2°C/60% RH ± 5% RH	0	Greyish black	Homogeneous	7.9±0.2	No progressions
		30	Greyish black	Homogeneous	7.5±0.2	No progressions
		60	Greyish black	Homogeneous	7.8±0.14	No progressions
		90	Greyish black	Homogeneous	7.9±0.61	No progressions
sGOPE	8°C ± 2°C/60% RH ± 5% RH	0	Greyish black	Homogeneous	6.8±0.6	No progressions
		30	Greyish black	Homogeneous	6.6±0.1	No progressions
		60	Greyish black	Homogeneous	6.6±0.2	No progressions
		90	Greyish black	Homogeneous	6.7±0.4	No progressions
GOPE	25°C ± 2°C/60% RH ± 5% RH	0	Greyish black	Homogeneous	7.9±0.2	No progressions
		30	Greyish black	Homogeneous	7.5±0.2	No progressions
		60	Greyish black	Homogeneous	7.6±0.5	No progressions
		90	Greyish black	Homogeneous	7.9±0.3	No progressions

sGOPE		0	Greyish black	Homogeneous	6.8±0.2	No progressions
		30	Greyish black	Homogeneous	6.9±0.2	No progressions
		60	Greyish black	Homogeneous	7.01±0.2	No progressions
		90	Greyish black	Homogeneous	7±0.2	No progressions
GOPE		0	Greyish black	Homogeneous	7.9±0.2	No progressions
		30	Greyish black	Homogeneous	7.9±0.2	No progressions
		60	Greyish black	Homogeneous	7.8±0.15	No progressions
		90	Greyish black	Homogeneous	7.8±0.4	No progressions
sGOPE	40°C ± 2°C/60% RH ± 5% RH	0	Greyish black	Homogeneous	6.8±0.2	No progressions
		30	Greyish black	Homogeneous	6.8±0.2	No progressions
		60	Greyish black	Homogeneous	6.7±0.32	No progressions
		90	Greyish black	Homogeneous	6.7±0.54	No progressions

CHAPTER- 7
CONCLUSION

CHAPTER-7

CONCLUSION

In the current examination work, graphene oxide and its subordinates were utilized for expulsion of weighty metal particles from watery arrangements and decontamination procedures on skin. A novel compound, silanized graphene oxide was synthesized from graphene oxide using APTES (3-aminopropyltriethoxysilane) as a silane precursor. The incorporated sGO was then portrayed by FTIR analysis, Thermogravimetric analysis (TGA), SEM analysis and Raman spectroscopy. FTIR analysis showed the peak of silane functional group indicating that the synthesized sGO is of good quality. Thermogravimetric analysis (TGA) analysis showed gradual changes in the sGO thermograms indicating higher stability compared to GO under thermal conditions. The SEM analysis of GO revealed rough, layered sheets with creased and crumpled edges, indicating the presence of functional groups. The increased number of wrinkles in sGO could be due to the presence of APTES between the layers i.e. due to silanization. In the Raman spectra of GO, band intensity ratio (I_D/I_G) of 0.84 is observed and in that of sGO spectra I_D/I_G ratio is 0.91. The expansion in the I_D/I_G proportion from 0.84 for GO to 0.91 for sGO indicates greater structural disorder and deformation of the graphene layers after silanization with APTES.

Adsorptive removal of heavy metal ions was assessed using sGO as adsorbent by Atomic absorption spectroscopy (AAS). The effect of dose experiment showed that sGO have good adsorption efficacy and shows better adsorptive removal of cobalt ions i.e. 85.29% than strontium ions which is 79.80% from the aqueous solution of heavy metal ions. The effect of contact time experiment showed that the adsorption process reaches equilibrium for both ions around after three to four hours. This indicates that sGO can be a promising material for the expulsion of these weighty metal particles, with Co^{2+} being slightly more efficiently removed than Sr^{2+} .

Fluorescence spectroscopy was carried out to study the complexation between sGO and heavy metal ions. The addition of metal ions (Co^{2+} and Sr^{2+}) to the sGO solution results

in an increase in fluorescence intensity. This increase in fluorescence intensity indicates that the metal ions are binding to the free surface of sGO.

Further, GO and sGO based topical pickering emulgel formulations were synthesized using adipate oil, kolliphorel, xanthum gum and glycerol as excipients for decontamination of simulants of heavy metal ions. The synthesized emulgels were characterized by physical appearance, Zeta, DLS, Optical microscopy, FTIR, contact angle, FE-SEM and DSC. Further rheological properties were analyzed using rheometer. The stability study was also performed for three-months under different temperature (4°C, 25°C and 40°C).

The synthesized emulgels appeared to be greyish-black in color, odorless and have smooth texture. The pH of sGOPE was found to be 6.08 ± 0.02 and that of GOPE was 7.9 ± 0.003 . The zeta potential of GOPE was found to be $-21.5 \pm 2.5\text{mV}$ and that of sGOPE was -18.5mV , which indicates that droplets of GOPE have negative charge which is closer to range where stable PE is formed. The DLS of GOPE revealed the size to be 518.9 nm and that of sGOPE was found to be 962nm.

Optical microscopy images revealed the even distribution of GO and sGO particles in the emulgel and homogenous preparation.

Rheological properties of the formulated emulgels indicated that they do not follow the Newton's law of viscosity indicating the non-newtonian and shear thinning flow behavior of the emulgels. Frequency sweep plot indicated the presence of stable gel-like formulation in the emulgels. Amplitude sweep plot indicated that the formulated emulgel exhibited viscoelastic solid properties ($G' > G''$) suggesting physical stability.

DSC analysis indicated that if temperature is increased above 119°C then formulation changes to molten state. The results of DSC indicated better stability of sGOPE as compared to GOPE.

FTIR spectra of GOPE and sGOPE illustrated that it contains the individual peaks of all the excipients used in the formulation of emulgels indicating the formation of proper emulgels.

The obtained contact angle (θ) for GO-based Pickering emulgel was 52.1° , while for sGO-based Pickering emulgel, it was 48.2° . These values suggest that the formed Pickering emulgels are of oil-in-water type, as value of θ for both the emulgels is less than 90° .

FE-SEM analysis of GOPE showed that particles of the formulation were discrete and longitudinal in shape with slight aggregation and that of sGOPE illustrated that particles have short curvy stretches at the surface.

The stability studies were indicative of stable nature of emulgel with no changes observed in appearance, minor pH variations and no phase separation was observed.

CHAPTER-8
FUTURE PROSPECTS

CHAPTER-8

FUTURE PROSPECTS

The research conducted on GO and sGO has revealed that both materials hold significant potential as adsorbents for eliminating heavy metal particles from fluid arrangements. These compounds are particularly valuable for conducting decontamination procedures, including formulations suitable for application on human skin.

In future studies, we plan to examine how the convergence of heavy metal particles affects adsorption behavior both GO and sGO. Additionally, we will explore how different temperatures impact the adsorption process. Temperature variations can influence the kinetics and thermodynamics of adsorption, and understanding these effects will enable us to optimize the conditions for maximum removal efficiency. The pH of the arrangement is another component that affects adsorption efficacy. Therefore, we will examine how different pH levels influence the ability of GO and sGO to adsorb heavy metal ions. This study will help us determine the optimal pH conditions for the best performance of these adsorbents.

Furthermore, we aim to extend our research to practical applications by performing decontamination studies using emulgels synthesized from GO and sGO, referred to as GOPE and sGOPE, respectively. These emulgels will be tested for their effectiveness in removing heavy metal particles from the skin. The studies will be conducted on Sprague-Dawley (SD) rats to assess the safety and efficacy of the formulations. The goal is to develop a skin-safe and effective topical decontamination formulation that can be used in real-world scenarios, such as in cases of chemical exposure.

The potential for these formulations to be commercialized as part of a first aid kit for military personnel is a promising avenue for future development. Such kits could provide immediate and effective decontamination in the field, enhancing the safety and preparedness of soldiers exposed to hazardous materials. By focusing on both the

fundamental aspects of adsorption and the practical applications, this research aims to bridge the gap between laboratory studies and real-world solutions, ultimately contributing to public health and safety in environments where heavy metal exposure is a concern.

CHAPTER-9

BIBLIOGRAPHY

BIBLIOGRAPHY

1. Abdel-Raouf, N., Sholkamy, E. N., Bukhari, N., Al-Enazi, N. M., Alsamhary, K. I., Al-Khiat, S. H. A., & Ibraheem, I. B. M. (2022). Bioremoval capacity of Co+2 using Phormidium tenue and Chlorella vulgaris as biosorbents. *Environmental Research*, 204, 111630. <https://doi.org/10.1016/j.envres.2021.111630>
2. Ahmadpour, A., Zabihi, M., Tahmasbi, M., & Bastami, T. R. (2010). Effect of adsorbents and chemical treatments on the removal of strontium from aqueous solutions. *Journal of Hazardous Materials*, 182(1–3), 552–556. <https://doi.org/10.1016/j.jhazmat.2010.06.067>
3. Ahmed, S. A., Verma, S., Khan, S., & Sharma, A. (2022). Emulgel: A revolution in topical drug delivery system. *International Journal of Health Sciences*, 6(June), 10834–10856. <https://doi.org/10.53730/ijhs.v6ns4.10902>
4. Alam, S. N., Sharma, N., & Kumar, L. (2017). Synthesis of Graphene Oxide (GO) by Modified Hummers Method and Its Thermal Reduction to Obtain Reduced Graphene Oxide (rGO)*. *Graphene*, 06(01), 1–18. <https://doi.org/10.4236/graphene.2017.61001>
5. Ali, M. M. S., Abdel-Galil, E. A., & Hamed, M. M. (2020). Removal of strontium radionuclides from liquid scintillation waste and environmental water samples. *Applied Radiation and Isotopes*, 166. <https://doi.org/10.1016/j.apradiso.2020.109357>
6. Almilly, R. F. K., Alobaidy, A. A., & Alhassani, M. H. (2023). Saponification of Diethyl Adipate with Sodium Hydroxide Using Reactive Distillation. *Journal of Engineering*, 20(11), 20–34. <https://doi.org/10.31026/j.eng.2014.11.02>
7. Amer, H., Moustafa, W. M., Farghali, A. A., El Rouby, W. M. A., & Khalil, W. F. (2017). Efficient Removal of Cobalt(II) and Strontium(II) Metals from Water using Ethylene Diamine Tetra-acetic Acid Functionalized Graphene Oxide. *Zeitschrift Fur Anorganische Und Allgemeine Chemie*, 643(22), 1776–1784. <https://doi.org/10.1002/zaac.201700318>
8. Bao, Y., Xue, H., Yue, Y., Wang, X., Yu, H., & Piao, C. (2021). Preparation and characterization of pickering emulsions with modified okara insoluble dietary fiber. *Foods*, 10(12). <https://doi.org/10.3390/foods10122982>
9. Benson, M. K. D., Goodwin, P. G., & Brostoff, J. (1975). Metal sensitivity in patients with joint replacement arthroplasties. *British Medical Journal*, 4(5993), 374–375. <https://doi.org/10.1136/bmj.4.5993.374>
10. Berthomieu, C., & Hienerwadel, R. (2009). Fourier transform infrared (FTIR) spectroscopy. *Photosynthesis Research*, 101(2–3), 157–170. <https://doi.org/10.1007/s11120-009-9439-x>
11. Bings, N. H., Bogaerts, A., & Broekaert, J. A. C. (2008). Atomic spectroscopy. In *Analytical Chemistry* (Vol. 80, Issue 12, pp. 4317–4347).

- <https://doi.org/10.1021/ac8006297>
12. Bose, A., Thomas, I., & Abraham, E. (2018). International Journal of Advances in Pharmaceutical Analysis Fluorescence spectroscopy and its applications: A Review QR Code *Correspondence Info. *International Journal of Advances in Pharmaceutical Analysis*. <https://doi.org/10.7439/ijapa>
 13. Charles, S., Geusens, N., Vergalito, E., & Nys, B. (2020). Interpol review of gunshot residue 2016–2019. *Forensic Science International: Synergy*, 2(xxxx), 416–428. <https://doi.org/10.1016/j.fsisyn.2020.01.011>
 14. Chevalier, Y., & Bolzinger, M. A. (2013). Emulsions stabilized with solid nanoparticles: Pickering emulsions. *Colloids and Surfaces A: Physicochemical and Engineering Aspects*, 439, 23–34. <https://doi.org/10.1016/j.colsurfa.2013.02.054>
 15. Chowdhury, M. J., & Blust, R. (2011). Strontium. In *Fish Physiology* (Vol. 31, Issue PART B). [https://doi.org/10.1016/S1546-5098\(11\)31029-1](https://doi.org/10.1016/S1546-5098(11)31029-1)
 16. Curling, C. A. (2016). *Review of Radioisotopes as Radiological Weapons*.
 17. Czarnek, K., Terpilowska, S., & Siwicki, A. K. (2015). Selected aspects of the action of cobalt ions in the human body. In *Central European Journal of Immunology* (Vol. 40, Issue 2, pp. 236–242). Termedia Publishing House Ltd. <https://doi.org/10.5114/ceji.2015.52837>
 18. DAOOD, N. M., E JASSIM, Z., M GAREEB, M., & ZEKI, H. (2019). STUDYING THE EFFECT OF DIFFERENT GELLING AGENT ON THE PREPARATION AND CHARACTERIZATION OF METRONIDAZOLE AS TOPICAL EMULGEL. *Asian Journal of Pharmaceutical and Clinical Research*, 571–577. <https://doi.org/10.22159/ajpcr.2019.v12i3.31504>
 19. Darchini-Maragheh, E., Balali-Mood, M., Malaknezhad, M., & Mousavi, S. R. (2018). Progressive delayed respiratory complications of sulfur mustard poisoning in 43 iranian veterans, three decades after exposure. *Human and Experimental Toxicology*, 37(2), 175–184. <https://doi.org/10.1177/0960327117694072>
 20. De Cauwer, H., Barten, D. G., Tin, D., Mortelmans, L. J., Ciottone, G. R., & Somville, F. (2023). 50 Years of Terrorism against the Nuclear Industry: A Review of 91 Incidents in the Global Terrorism Database. *Prehospital and Disaster Medicine*, 38(2), 199–206. <https://doi.org/10.1017/S1049023X2300002X>
 21. Dieng, S. M., Omran, Z., Anton, N., Thioune, O., Djiboune, A. R., Sy, P. M., Messaddeq, N., Ennahar, S., Diarra, M., & Vandamme, T. (2020). Pickering nano-emulsions stabilized by Eudragit RL100 nanoparticles as oral drug delivery system for poorly soluble drugs. *Colloids and Surfaces B: Biointerfaces*, 191. <https://doi.org/10.1016/j.colsurfb.2020.111010>
 22. Domínguez-Gadea, L., & Cerezo, L. (2011). Decontamination of radioisotopes. In *Reports of Practical Oncology and Radiotherapy* (Vol. 16, Issue 4, pp. 147–152). Urban and Partner. <https://doi.org/10.1016/j.rpor.2011.05.002>
 23. Donald Barceloux, C. G., & Barceloux, D. (1999). For personal use only. In

- Clinical Toxicology* (Vol. 37, Issue 2). www.dekker.com
24. Donthi, M. R., Munnangi, S. R., Krishna, K. V., Saha, R. N., Singhvi, G., & Dubey, S. K. (2023). Nanoemulgel: A Novel Nano Carrier as a Tool for Topical Drug Delivery. *Pharmaceutics*, 15(1). <https://doi.org/10.3390/PHARMACEUTICS15010164>
 25. Dutta, A. (2017). Fourier Transform Infrared Spectroscopy. In *Spectroscopic Methods for Nanomaterials Characterization* (Vol. 2, pp. 73–93). Elsevier. <https://doi.org/10.1016/B978-0-323-46140-5.00004-2>
 26. Ebert, D. D., Nobis, S., Lehr, D., Baumeister, H., Riper, H., Auerbach, R. P., Snoek, F., Cuijpers, P., & Berking, M. (2017). The 6-month effectiveness of Internet-based guided self-help for depression in adults with Type 1 and 2 diabetes mellitus. *Diabetic Medicine*, 34(1), 99–107. <https://doi.org/10.1111/dme.13173>
 27. Edwards, C. A. (2002). *Assessing the effects of environmental pollutants on soil organisms, communities, processes and ecosystems*. www.elsevier.com/locate/ejsobi
 28. Einollahi Peer, F., Bahramifar, N., & Younesi, H. (2018). Removal of Cd (II), Pb (II) and Cu (II) ions from aqueous solution by polyamidoamine dendrimer grafted magnetic graphene oxide nanosheets. *Journal of the Taiwan Institute of Chemical Engineers*, 87, 225–240. <https://doi.org/10.1016/j.jtice.2018.03.039>
 29. Espert, M., Hernández, M. J., Sanz, T., & Salvador, A. (2022). Rheological properties of emulsion templated oleogels based on xanthan gum and different structuring agents. *Current Research in Food Science*, 5, 564–570. <https://doi.org/10.1016/j.crfs.2022.03.001>
 30. Etemad, L., Moshiri, M., & Balali-Mood, M. (2018). A Narrative Review of Recent Advances by Iranian Researchers Part II: Clinical Management and Therapy. In *Iran J Med Sci* (Vol. 43, Issue 3).
 31. Fosu, M. A., Ofori-Kwakye, K., Kuntworbe, N., & Bonsu, M. A. (2016). Investigation of blends of cashew and xanthan gums as a potential carrier for colonic delivery of Ibuprofen. *International Journal of PharmTech Research*, 9(7), 369–380.
 32. Fraga, L. G., Silva, J., Teixeira, S., Soares, D., Ferreira, M., & Teixeira, J. (2020). Influence of operating conditions on the thermal behavior and kinetics of pine wood particles using thermogravimetric analysis. *Energies*, 13(11), 1–22. <https://doi.org/10.3390/en13112756>
 33. Frelichowska, J., Bolzinger, M. A., Valour, J. P., Mouaziz, H., Pelletier, J., & Chevalier, Y. (2009). Pickering w/o emulsions: Drug release and topical delivery. *International Journal of Pharmaceutics*, 368(1–2), 7–15. <https://doi.org/10.1016/j.ijpharm.2008.09.057>
 34. Goel, R., Bhardwaj, S., & Bana, S. (2023). Pharmaceutical excipients. *Dosage Forms, Formulation Developments and Regulations: Recent and Future Trends in Pharmaceutics, Volume 1, 1*, 311–348. <https://doi.org/10.1016/B978-0-323-91817-6.00003-6>

35. Gruss, I., Stefanovska, T., Twardowski, J., Pidlisnyuk, V., & Shapoval, P. (2019). The ecological risk assessment of soil contamination with Ti and Fe at military sites in Ukraine: avoidance and reproduction tests with *Folsomia candida*. *Reviews on Environmental Health*, 34(3), 303–307. <https://doi.org/10.1515/reveh-2018-0067>
36. Huo, J., Yu, G., & Wang, J. (2021). Efficient removal of Co(II) and Sr(II) from aqueous solution using polyvinyl alcohol/graphene oxide/MnO₂ composite as a novel adsorbent. *Journal of Hazardous Materials*, 411. <https://doi.org/10.1016/j.jhazmat.2021.125117>
37. Hurst, C. G. (n.d.). *Chapter 15 DECONTAMINATION INTRODUCTION METHODS OF DECONTAMINATION Physical Removal Chemical Methods Certification of Decontamination WOUND DECONTAMINATION Initial Decontamination General Considerations Thickened Agents Off-Gassing Foreign Material Wound Contamination Assessment Dilute Hypochlorite Solution Wound Exploration/Debridement BIOLOGICAL AGENT DECONTAMINATION Chemical Method Physical Method SUMMARY.*
38. Jaishankar, M., Tseten, T., Anbalagan, N., Mathew, B. B., & Beeregowda, K. N. (2014). Toxicity, mechanism and health effects of some heavy metals. In *Interdisciplinary Toxicology* (Vol. 7, Issue 2, pp. 60–72). Slovak Toxicology Society. <https://doi.org/10.2478/intox-2014-0009>
39. Järup, L. (2003). Hazards of heavy metal contamination. In *British Medical Bulletin* (Vol. 68, pp. 167–182). <https://doi.org/10.1093/bmb/ldg032>
40. Jiang, Y., Yan, S., Chen, Y., & Li, S. (2019). Preparation, characterization, and properties of silanized graphene oxide reinforced biobased benzoxazine-bismaleimide resin composites. *Journal of Adhesion Science and Technology*, 33(18), 1974–1988. <https://doi.org/10.1080/01694243.2019.1623434>
41. Jiříčková, A., Jankovský, O., Sofer, Z., & Sedmidubský, D. (2022). Synthesis and Applications of Graphene Oxide. In *Materials* (Vol. 15, Issue 3). MDPI. <https://doi.org/10.3390/ma15030920>
42. kabita sharma 2023. (n.d.).
43. Karakurt, S., & Baş, K. (2024). KİMYASAL, BİYOLOJİK, RADYOLOJİK ve NÜKLEER (KBRN) OLAYLARI İÇİN DEKONTAMİNASYON SOLÜSYONLARI ve TEKNİKLERİ. *Savunma Bilimleri Dergisi*, 20(1), 29–48. <https://doi.org/10.17134/khosbd.1360355>
44. Koilraj, P., Kamura, Y., & Sasaki, K. (2018). Cosorption Characteristics of SeO₄²⁻ and Sr²⁺ Radioactive Surrogates Using 2D/2D Graphene Oxide-Layered Double Hydroxide Nanocomposites. *ACS Sustainable Chemistry and Engineering*, 6(11), 13854–13866. <https://doi.org/10.1021/acssuschemeng.8b02056>
45. Li, Y., Wang, M., Guan, D., Lv, H., Zhao, J., Yu, X., Yang, X., & Wu, C. (2017). A Study on the Decontaminated Efficiency of Ultraviolet Device on the Indoor Airborne Bacteria. *Procedia Engineering*, 205, 1376–1380. <https://doi.org/10.1016/j.proeng.2017.10.281>

46. Li, Y., & Xiang, D. (2019). Stability of oil-in-water emulsions performed by ultrasound power or high-pressure homogenization. *PLoS ONE*, *14*(3). <https://doi.org/10.1371/journal.pone.0213189>
47. Mishra, J., Saini, R., & Singh, D. (2021). Review paper on removal of heavy metal ions from industrial waste water effluent. *IOP Conference Series: Materials Science and Engineering*, *1168*(1), 012027. <https://doi.org/10.1088/1757-899x/1168/1/012027>
48. Mohamed, M. A., Jaafar, J., Ismail, A. F., Othman, M. H. D., & Rahman, M. A. (2017). Fourier Transform Infrared (FTIR) Spectroscopy. In *Membrane Characterization* (pp. 3–29). Elsevier Inc. <https://doi.org/10.1016/B978-0-444-63776-5.00001-2>
49. Mohite, S. V., Salunkhe, A. K., & Sudke, Suresh G. (2019). Emulgel: A Novel Approach For Hydrophobic Drugs. *American Journal of PharmTech Research*, *9*(2), 208–224. <https://doi.org/10.46624/ajptr.2019.v9.i2.018>
50. Moraes, L. R. d. C., Ribeiro, H., Cargnin, E., Andrade, R. J. E., & Naccache, M. F. (2020). Rheology of graphene oxide suspended in yield stress fluid. *Journal of Non-Newtonian Fluid Mechanics*, *286*. <https://doi.org/10.1016/j.jnnfm.2020.104426>
51. Naresh, K. (n.d.). *National Level Workshop on Spectroscopic Techniques in Structural Elucidation Journal of Chemical and Pharmaceutical Sciences Applications of Fluorescence Spectroscopy*. www.jchps.com
52. Ouyang, Y., Deng, J., Chen, Z., Yang, L., Xiao, S., Wang, L., & Zhao, Y. (2020). Preparation and assessment of magnetic graphene oxide/chitosan composite for removing radiocobalt from aqueous solution. *Journal of Radioanalytical and Nuclear Chemistry*, *326*(3), 1699–1708. <https://doi.org/10.1007/s10967-020-07462-5>
53. Payne, L. R. (1977). The Hazards of Cobalt*. In *J. Soc. Occup. Med* (Vol. 27). <http://ocmed.oxfordjournals.org/>
54. Platt, P. (1971). Atomic absorption spectroscopy. *Selected Annual Reviews of the Analytical Sciences, I*, 177–234. <https://doi.org/10.1039/AS9710100177>
55. Prasad, Pbn., & Krishna, Bc. (n.d.). *Pincode-523370 2 B.Pharmacy, Sankar Reddy Institute of Pharmaceutical Sciences*. 523370. <https://doi.org/10.37022/jis.v6i3.62>
56. Prodan, D., Moldovan, M., Furtos, G., Saroși, C., Filip, M., Perhaița, I., Carpa, R., Popa, M., Cuc, S., Varvara, S., & Popa, D. (2021). Synthesis and characterization of some graphene oxide powders used as additives in hydraulic mortars. *Applied Sciences (Switzerland)*, *11*(23). <https://doi.org/10.3390/app112311330>
57. Qasem, N. A. A., Mohammed, R. H., & Lawal, D. U. (2021). Removal of heavy metal ions from wastewater: a comprehensive and critical review. *Npj Clean Water*, *4*(1). <https://doi.org/10.1038/s41545-021-00127-0>
58. Rana, S., Sharma, N., Ojha, H., Shivkumar, H. G., Sultana, S., & Sharma, R. K. (2014a). P-Tertbutylcalix[4]arene nanoemulsion: Preparation, characterization

- and comparative evaluation of its decontamination efficacy against Technetium-99m, Iodine-131 and Thallium-201. *Colloids and Surfaces B: Biointerfaces*, 117, 114–121. <https://doi.org/10.1016/j.colsurfb.2014.02.001>
59. Rana, S., Sharma, N., Ojha, H., Shivkumar, H. G., Sultana, S., & Sharma, R. K. (2014b). P-Tertbutylcalix[4]arene nanoemulsion: Preparation, characterization and comparative evaluation of its decontamination efficacy against Technetium-99m, Iodine-131 and Thallium-201. *Colloids and Surfaces B: Biointerfaces*, 117, 114–121. <https://doi.org/10.1016/j.colsurfb.2014.02.001>
 60. Research, O. •, Group, •, & Barnaby, F. (2005). *Dirty Bombs and Primitive Nuclear Weapons*. www.oxfordresearchgroup.org.uk.
 61. Shukla, Saurabh, Grace Mbingwa, Sakshum Khanna, Jyoti Dalal, Deeksha Sankhyan, Anindita Malik, and Neha Badhwar. "Environment and health hazards due to military metal pollution: A review." *Environmental Nanotechnology, Monitoring & Management* (2023): 100857.
 62. Skalny, A. V., Aschner, M., Bobrovniksky, I. P., Chen, P., Tsatsakis, A., Paoliello, M. M. B., Buha Djordevic, A., & Tinkov, A. A. (2021). Environmental and health hazards of military metal pollution. In *Environmental Research* (Vol. 201). Academic Press Inc. <https://doi.org/10.1016/j.envres.2021.111568>
 63. Sriandhal Sabalingam, & Malitha Aravinda Siriwardhene. (2022). A review on emerging applications of emulgel as topical drug delivery system. *World Journal of Advanced Research and Reviews*, 13(1), 452–463. <https://doi.org/10.30574/wjarr.2022.13.1.0048>
 64. Szymańska, E., Potaś, J., Maciejczyk, M., Sulewska, M. E., Pietruska, M., Zalewska, A., Pietruska, A., & Winnicka, K. (2023). Preliminary Assessment of Polysaccharide-Based Emulgels Containing Delta-Aminolevulinic Acid for Oral Lichen planus Treatment. *Pharmaceuticals*, 16(11). <https://doi.org/10.3390/ph16111534>
 65. Talmage, S. S., Watson, A. P., Hauschild, V., Munro, N. B., & King, J. (2007). Chemical Warfare Agent Degradation and Decontamination. In *Current Organic Chemistry* (Vol. 11).
 66. Tang, M., Wu, T., Xu, X., Zhang, L., & Wu, F. (2014). Factors that affect the stability, type and morphology of Pickering emulsion stabilized by silver nanoparticles/graphene oxide nanocomposites. *Materials Research Bulletin*, 60, 118–129. <https://doi.org/10.1016/j.materresbull.2014.08.019>
 67. Tayyebi, A., Outokesh, M., Moradi, S., & Doram, A. (2015). Synthesis and characterization of ultrasound assisted “graphene oxide-magnetite” hybrid, and investigation of its adsorption properties for Sr(II) and Co(II) ions. *Applied Surface Science*, 353, 350–362. <https://doi.org/10.1016/j.apsusc.2015.06.087>
 68. Tomonaga, M. (2019). The Atomic Bombings of Hiroshima and Nagasaki: A Summary of the Human Consequences, 1945-2018, and Lessons for Homo sapiens to End the Nuclear Weapon Age. In *Journal for Peace and Nuclear Disarmament* (Vol. 2, Issue 2, pp. 491–517). Routledge.

- <https://doi.org/10.1080/25751654.2019.1681226>
69. Toorchi, D., Tohidlou, E., & Khosravi, H. (2022). Enhanced flexural and tribological properties of basalt fiber-epoxy composite using nano-zirconia/graphene oxide hybrid system. *Journal of Industrial Textiles*, 51(2), 3238S-3252S. <https://doi.org/10.1177/1528083720920573>
 70. Trovo, P. L. V., Fregolente, L. G., Amaral, C. D. B., & Gonzalez, M. H. (2017). Determination of vanadium in water samples from Brazilian mineral spring (Ibirá Spa) using ICP-MS. *Environmental Nanotechnology, Monitoring and Management*, 8, 48–52. <https://doi.org/10.1016/j.enmm.2017.04.005>
 71. Vanpariya, F., Shiroya, M., & Malaviya, M. (2021). *Emulgel : A Review*. April. <https://doi.org/10.21275/SR21311095015>
 72. Vidu, R., Matei, E., Predescu, A. M., Alhalaili, B., Pantilimon, C., Tarcea, C., & Predescu, C. (2020). Removal of heavy metals from wastewaters: A challenge from current treatment methods to nanotechnology applications. *Toxics*, 8(4), 1–37. <https://doi.org/10.3390/toxics8040101>
 73. Vipin, A. K., Ling, S., & Fugetsu, B. (2016). Removal of Cs⁺ and Sr²⁺ from water using MWCNT reinforced Zeolite-A beads. *Microporous and Mesoporous Materials*, 224, 84–88. <https://doi.org/10.1016/j.micromeso.2015.11.024>
 74. Vukašinić, M., Pantelić, I., Savić, S., Cekić, N., Vukašinić Sekulić, M., Antić Stanković, J., Božić, D. D., Tošić, A., Tamburić, S., & Savić, S. D. (2023). Development of a “Green” Emulsion with a Milk Protein Hydrolysate: An Evaluation of Rheology, Texture, In Vitro Bioactivity, and Safety. *Cosmetics*, 10(6). <https://doi.org/10.3390/cosmetics10060162>
 75. Vuppalladadiam, S. S. R., Agarwal, T., Kulanthaivel, S., Mohanty, B., Barik, C. S., Maiti, T. K., Pal, S., Pal, K., & Banerjee, I. (2020). Silanization improves biocompatibility of graphene oxide. *Materials Science and Engineering C*, 110. <https://doi.org/10.1016/j.msec.2020.110647>
 76. Warning, S. (2018). *SCIENCE & ENGINEERING*. 63628.
 77. Xing, M., Zhuang, S., & Wang, J. (2019). Adsorptive removal of strontium ions from aqueous solution by graphene oxide. *Environmental Science and Pollution Research*, 26(29), 29669–29678. <https://doi.org/10.1007/s11356-019-06149-z>
 78. Xu, S., & Dodt, A. (2023). Nuclear bomb and public health. *Journal of Public Health Policy*, 44(3), 348–359. <https://doi.org/10.1057/s41271-023-00420-x>
 79. Yusof, N. F., Mehamod, F. S., & Mohd Suah, F. B. (2019). Fabrication and binding characterization of ion imprinted polymers for highly selective Co²⁺ ions in an aqueous medium. *Journal of Environmental Chemical Engineering*, 7(2), 103007. <https://doi.org/10.1016/j.jece.2019.103007>
 80. Zhuang, S., & Wang, J. (2023). Efficient adsorptive removal of Co²⁺ from aqueous solution using graphene oxide. *Environmental Science and Pollution Research*, 30(45), 101433–101444. <https://doi.org/10.1007/s11356-023-29374-z>

saumya thesis.docx

ORIGINALITY REPORT

3%

SIMILARITY INDEX

PRIMARY SOURCES

1	sciencescholar.us Internet	131 words — 1%
2	www.ncbi.nlm.nih.gov Internet	124 words — 1%
3	Min Xing, Shuting Zhuang, Jianlong Wang. "Adsorptive removal of strontium ions from aqueous solution by graphene oxide", <i>Environmental Science and Pollution Research</i> , 2019 Crossref	47 words — < 1%
4	Abdul Khan, Sabna Kotta, Shahid Ansari, Javed Ali, Rakesh Sharma. "Recent Advances in Decontamination of Chemical Warfare Agents", <i>Defence Science Journal</i> , 2013 Crossref	29 words — < 1%
5	essuir.sumdu.edu.ua Internet	16 words — < 1%
6	Aastha Dutta. "Fourier Transform Infrared Spectroscopy", Elsevier BV, 2017 Crossref	14 words — < 1%
7	Pradeep Kumar, Harpreet Singh, Meghna Kapur, Monoj Kumar Mondal. "Comparative study of malathion removal from aqueous solution by agricultural and	14 words — < 1%



1st INTERNATIONAL CONFERENCE
ON

RECENT ADVANCEMENTS IN APPLIED SCIENCES AND TECHNOLOGY
(ICRAAST 2024)

(May 29-31, 2024)

CERTIFICATE OF PRESENTATION

Ref. No.:

Date: 31/05/2024

This is to certify that Prof./Dr./Mr./Ms. Saumya Tomel from Innovative College of Pharmacy Greater Noida has presented (Oral/Poster) his /her work entitled "Synthesis and characterization of Graphene oxide based Pickering " at International Conference on Recent Advancements in Applied Sciences and Technology organized by the Applied Science Cluster, UPES, Dehradun, India.


Prof. Ranjeet Brajpurriya
Co-Chairman


Prof. Shalendra Kumar
Convener



Contact

Phone

+91-9811131924

Address

HS-1, 44, Uday Homes, Ghaziabad,
UP-201005

Education

2022-2024

Masters of Pharmacy Sem (1, 2 & 3)- 88.6%

Dr. A.P.J. Abdul Kalam Technical
University

2019-2022

Bachelors of Pharmacy - 75.6%
Delhi Pharmaceutical Sciences and
Research University

2017-2019

Diploma of Pharmacy - 78%
Delhi Pharmaceutical Sciences and
Research University

2017

**Senior Secondary Education, XII
- 88.2%**
Greenfields Public School

2015

Secondary Education, X - 10 CGPA
Greenfields Public School

Skills

- **Technical:** UV spectrophotometry, FT-IR, Fluorescence spectroscopy, SAS (Base)
- **Software:** Origin, ChemDraw, BioRender, MS Office
- **Soft:** Adaptability, empathy, critical thinking, decision-making

Reference

Letter of recommendation from Dr.
Himanshu Ojha, Scientist 'F',
Department of CBRN, INMAS, DRDO

SAUMYA TOMER

tomersaumya@gmail.com | <https://www.linkedin.com/in/saumya-tomer-571301218>

Master of Pharmacy candidate proficient in advanced pharmaceutical instrumentation and laboratory experiments, committed to innovative pharmaceutical solutions.

Internships

○ January 2024 - June 2024

Institute of Nuclear Medicine and Allied Sciences, DRDO, New Delhi
Research Scholar

- Executed dissertation work for the completion of Masters of Pharmacy
- Leads on training on: UV spectrophotometer, Fluorescence spectrometer, FT-IR
- Animal handling and experiments on them
- Learned software including CHEMDRAW, ORIGIN, BIORENDER

○ May 2019 - August 2019

Charak Palika Hospital, NDMC
Hospital Trainee

- Completed 500 hours practical training under Pharmacy department
- Patient counselling on new medications and OTC drugs
- Updated patient profiles
- Prescription reading and dispensing

Projects

- Comparative quality control tests of different brands of calcium and vitamin D tablets
- Pharmacovigilance: History, importance, current scenarios, future prospects
- Determination of efficacy of graphene oxide and silanized graphene oxide based topical pickering emulgel for the removal of heavy metal ions

Publication

- Formulation and in-vitro evaluation of meloclopramide microspheres in EBPS

Achievements

- Poster presentation on topic "Synthesis and characterization of Graphene Oxide based Pickering emulgel formulation against CBRN agents" at 1st International Conference on Recent Advances in Applied Sciences organized by UPES, Dehradun - (29-31 May, 2024)
- Presented oral abstract presentation on the topic "Formulation and characterization of Pistia striatiotes herbal cream for eczema" at International Conference organized by Lloyd - (9 Dec, 2023)
- Academic topper in B.Pharm 5th semester - **Gold medalist**
- Secured 3rd rank in Diploma in Pharmacy

Conferences

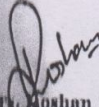
- International Conference themed "Recent Advances in Applied Sciences" at: UPES, Dehradun (28-31 May, 2024)
- International Conference themed "Transformation through Technology and Transdisciplinary Education" at Lloyd Institute (9 Dec, 2023)
- Exhibition by INMAS - DRDO achievements in last 9 years (8 July, 2023)
- Pharmacovigilance workshop cum Industrial training at Jramin Hamdard (16 Feb, 2023)

Certifications

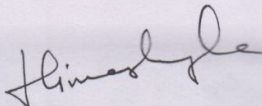
- Certificate of participation in National Workshop on "Fundamental techniques of animal handling and restraining of animal" at Innovative College of Pharmacy - (8 April, 2024)
- Certificate of participation of oral abstract presentation at International conference at Lloyd Institute.
- Certificate of training in SAS (BASE) for successfully completing the program - (12 March, 2023)
- Diligent trainee certification from Charak Palika Hospital (NDMC)
- Certificate of achievement- PHARMA QUIZ OF 1ST 2K 20 - (7 May, 2022)

CERTIFICATE-I

Certified that **Saumya Tomer** (2202270566005) has carried out the research work presented in this thesis entitled "**Decontamination efficacy of graphene oxide and silanized graphene oxide based topical Pickering emulgels for removal of heavy metal ions**" for the award of **Master of Pharmacy** from Dr. APJ Abdul Kalam Technical University, Lucknow under our supervision in collaboration with **Institute of Nuclear Medicine & Allied Sciences (INMAS), DRDO**. The thesis embodies results of original work, and studies are carried out by the student herself and the contents of the thesis do not form the basis for the award of any other degree to the candidate or anyone else from this or any other university/institution.


Mr. Ashan Zehra
Associate Professor
Innovative College of Pharmacy
Greater Noida, UP-201308




Dr. Himanshu Ojha
Scientist 'F'
Department of CBRN
INMAS, DRDO

Mrs. Nandhya Sharma
Assistant Professor
Innovative College of Pharmacy
Greater Noida, UP-201308

Date :